Eine erhöhte beta2-adrenerge Signalübertragung fördert die Frakturheilung durch Kallus-Neovaskularisation in Mäusen

Dissertation

zur Erlangung des akademischen Grades eines

Doktors der Medizin (Dr. med.)

an der

Medizinischen Fakultät der Universität Hamburg

vorgelegt von

Paul Richard Johannes Knapstein

aus

Mainz

2024

Angenommen von der Medizinischen Fakultät am: **08.04.2025**

Veröffentlicht mit Genehmigung der Medizinischen Fakultät der Universität Hamburg

Betreuer:in / Gutachter:in der Dissertation: **Prof. Dr. Dr. Johannes Keller**

Gutachter:in der Dissertation: **Prof. Dr. Sandra Pohl**

Vorsitz der Prüfungskommission: **Prof. Dr. Sandra Pohl**

Mitglied der Prüfungskommission: **PD Dr. Dr. Tim Rolvien**

Mitglied der Prüfungskommission: **Prof. Dr. Maike Frye**

Datum der mündlichen Prüfung: **08.04.2025**

INHALTSVERZEICHNIS

1. Darstellung der Publikation

Jahn D*, **Knapstein PR***, Otto E*, Köhli P*, Sevecke J, Graef F, Graffmann C, Fuchs M, Jiang S, Rickert M, Erdmann C, Appelt J, Revend L, Küttner Q, Witte J, Rahmani A, Duda G, Xie W, Donat A, Schinke T, Ivanov A, Tchouto MN, Beule D, Frosch KH, Baranowsky A, Tsitsilonis S, Keller J. Increased β2-adrenergic signaling promotes fracture healing through callus neovascularization in mice. Sci Transl Med. 2024 Apr 17;16(743):eadk9129. doi: 10.1126/scitranslmed.adk9129. Epub 2024 Apr 17. PMID: 38630849. **contributed equally*

1.1. Einleitung

Das Skelett bildet die Grundlage für den anatomischen Aufbau aller Säugetiere und vieler weiterer Lebensarten. Hierbei ist das Knochensystem nicht nur essenziell für die Fortbewegung, den Schutz von Organen und Stabilität des Körpers, sondern auch zentraler Regulator für die Speicherung von Mineralien, der Hämatopoese und diverser metabolischer Prozesse. Daher ist der Knochen heute als endokrines Organ anerkannt [1,2]. Die Effektivität von Knochenumbau und der narbenlosen Regeneration nach einer Verletzung haben sich im Verlauf der evolutionären Entwicklung hinweg erhalten. Das Gewebe bleibt durch seinen dynamischen Umbauprozess, dem „Remodeling“, permanent an interne und externe Bedingungen anpassungsfähig. Sowohl das Remodeling als auch die Regeneration nach einer Verletzung werden durch die koordinierte Aktivität der knochenabbauenden Osteoklasten und den knochenbildenden Osteoblasten erreicht [3]. Der Knochen wird zusätzlich von der Knochenhaut, dem Periost, umgeben, das durch eine Vielzahl von Stammzellen, Nerven und Gefäßen eine regenerative und ernährende Funktion besitzt und darüber hinaus nach einer Knochenverletzung die Neovaskularisation des Kallus mit osteogenen Typ-H-Gefäßen fördert [4,5].

Aufgrund des demographischen Wandels mit steigender Lebenserwartung sind wir heutzutage mit einer hohen Inzidenz von Skeletterkrankungen konfrontiert [6,7]. Bei Frauen entspricht das Risiko einer osteoporotischen Fraktur dem kombinierten Risiko von Brust-, Gebärmutter- und Eierstockkrebs [7]. Fast 24 % der Patienten mit Hüftfrakturen im Alter von über 50 Jahren versterben innerhalb eines Jahres [7]. Auch nach einer Fraktur, die adäquat durch bewährte Verfahren behandelt wurde, besteht immer noch ein Risiko von bis zu 15 %, dass der Knochen sechs Monate nach Verletzung nicht ausreichend heilt, was als Pseudarthrose definiert wird [3]. Diese gestörte Frakturheilung stellt eine erhebliche Belastung für die Patienten dar, die sich häufig wiederholten Revisionsoperationen unterziehen müssen, was zu weiteren Komplikationen führen

kann. Dies führt zu längerer Immobilisierung, Behinderung oder sogar zum Tod [8] und verursacht insgesamt hohe sozioökonomische Kosten.

In diesem Zusammenhang wurde das sympathische Nervensystem (SNS) und sein wichtigstes Effektormolekül, Noradrenalin (Norepinephrin; NE), als essenzieller Regulator des Knochenumbaus identifiziert. Nach Bindung von NE an den G-Protein-gekoppelten beta2-adrenergen Rezeptor (Adrb2) wird die Knochenbildung gehemmt und die Knochenresorption gefördert [9,10]. Zwar ist diese hemmende Auswirkung des Sympathikus auf den Knochenumbau im intakten Skelett inzwischen gut erforscht, aber es blieb bisweilen unklar, inwiefern diese Signalwege auch die Knochenregeneration nach einer Verletzung modulieren.

Anhand eines zuvor veröffentlichten Modells [11], bei dem eine Femurosteotomie mit einem externen Fixateur stabilisiert wird, demonstriert die vorliegende Studie, dass das sympathische Nervensystem maßgeblich die Frakturheilung über Adrb2 in adulten Mäusen beeinflusst. Während der Heilung von Knochenbrüchen führt die Aktivierung von Adrb2 in Periostzellen und Osteoblasten zu einer erhöhten Expression des vaskulären endothelialen Wachstumsfaktors A (Vegfa). Dies resultiert in einer verstärkten Bildung von osteogenen Typ-H-Gefäßen und somit zu einer verbesserten Vaskularisation des Frakturkallus. Obwohl Adrb2 bei ansonsten gesunden und jungen Mäusen nur eine untergeordnete Rolle bei der Knochenheilung spielt, fördert er insbesondere bei adulten Mäusen mit physiologisch erhöhtem Sympathikotonus die Knochenregeneration. Aus translationaler Sicht führt die systemische Behandlung mit dem Adrb2-Antagonisten Propranolol zu einer gestörten Knochenheilung, während die Behandlung mit dem Adrb2-Agonisten Formoterol in einer gesteigerten Neovaskularisation und verbesserten Knochenregeneration resultiert. Die vorliegenden Ergebnisse identifizieren eine bislang unbekannte Rolle von Adrb2 in der Frakturheilung, die pharmakologisch zur Therapie der gestörten Knochenheilung genutzt werden könnte.

1.2. Ergebnisse

Der Adrb2-Rezeptor zeigt einen altersabhängigen Einfluss auf den Knochenumbau und die Regeneration

Um die Rolle des SNS und seinem Rezeptor Adrb2 im Skelettsystem zu charakterisieren, wurden junge (12 Wochen alt, niedriger Sympathikotonus) und gealterte (30 Wochen alt, physiologisch erhöhter Sympathikotonus) Adrb2-defiziente Mäuse untersucht. Hier wurden zunächst der Knochenumbau und die Knochenregeneration in 12 Wochen alten Mäusen analysiert. Die histologische Auswertung des nicht-frakturierten Skeletts zeigte, dass in diesem Alter kein Unterschied in der Knochenarchitektur oder dem zellulären Remodeling zwischen *Adrb2*$^{+/+}$ und *Adrb2*$^{-/-}$ Mäusen zu beobachten ist. Auch die radiologische Untersuchung mittels mikro-Computertomographie (µCT) zeigte keine Unterschiede in der Knochenregeneration 7, 14 und 21 Tage nach Femurosteotomie. Demnach spielen das SNS und Adrb2 in jungen Mäusen mit niedrigem Sympathikotonus nur eine untergeordnete Rolle in der Regulation des Knochenumbaus und in der Knochenheilung.

Im Gegensatz hierzu wiesen *Adrb2*$^{-/-}$ Mäuse im Alter von 30 Wochen (im Folgenden als adulte Mäuse bezeichnet) eine gesteigerte Knochenmasse im nicht-frakturierten Skelett auf. Die Histologie der Wirbelsäule demonstrierte eine erhöhte Trabekeldicke, was durch eine erhöhte Knochenbildung bei reduzierter Knochenresorption erklärt werden konnte. Auch im nicht-frakturierten, distalen Femur konnte ein erhöhtes Knochenvolumen in der *Adrb2*$^{-/-}$ Kohorte im Vergleich zu den Wildtyp (WT) Wurfgeschwistern beobachtet werden. Im Gegensatz zum nicht-frakturierten Skelett zeigten die radiologischen und histologischen Analysen eine unerwartete und stark beeinträchtigte Knochenheilung in adulten *Adrb2*$^{-/-}$ Tieren 7 und 14 Tage nach Femurosteotomie. Dies führte an Tag 21 nach Femurosteotomie zu einer unzureichenden Knochenheilung mit einer hohen Rate an atrophen Pseudarthrosen. Histomorphometrische Untersuchungen mittels Tartrat-resistenter saurer Phosphatase (TRAP) und Toluidin-Blau-Färbungen zeigten zu diesem Zeitpunkt eine Abnahme sowohl der Osteoklasten- als auch der Osteoblasten-Parameter im Kallus der adulten *Adrb2*$^{-/-}$ Mäuse. Die unzureichende Bildung neuen Knochens im Frakturspalt konnte mittels Quantifizierung der Calcein-Inkorporation im heilenden Knochen bestätigt werden. Zusammengenommen deuten diese Daten erstmalig darauf hin, dass das SNS und Adrb2 im adulten Organismus einen differentiellen Einfluss auf das Skelettsystem ausüben. Während im nicht-frakturierten Skelett Adrb2 die Knochenmasse erniedrigt, ist Adrb2 von essenzieller Bedeutung für die adäquate Heilung des frakturierten Knochens.

Erhöhter Sympathikotonus im Knochen adulter Mäuse

Die Untersuchung von jungen und adulten Mäusen zeigten einen altersabhängigen Einfluss von Adrb2 auf die Knochenheilung. Als mögliche Erklärung zeigten vorherige Studien, dass der Grundtonus des Sympathikus physiologisch mit zunehmendem Alter ansteigt [12]. Demnach wurde die Aktivität des SNS mittels Surrogatparametern systemisch und lokal analysiert. Die Messung des stabilen NE-Metaboliten, Normetanephrin, zeigte jedoch keinen Unterschied zwischen jungen und adulten WT-Mäusen im Serum. Allerdings war die Expression des transmembranären NE-Transporters, welcher die Wiederaufnahme von NE in die Knochenzellen vermittelt und von dem *Slc6a2*-Gen (Solute Carrier Family 6 Member 2) kodiert wird, bei adulten Mäusen stark reduziert. Die geringe Genexpressionsrate von *Slc6a2* im adulten Skelett führte zu einem erhöhten Gesamt-NE-Gehalt im Femur. Das Skelett der 12 Wochen alten Tiere zeigte hingegen eine hohe Expression von *Slc6a2*, was mit einer hohen Wiederaufnahme in die Zellen und folglich mit einer verminderten extrazellulärer Gesamtkonzentration von NE im Knochen assoziiert war. Demnach ist davon auszugehen, dass die altersabhängige Expression von *Slc6a2* im Knochen die lokalen NE-Spiegel reguliert und somit entscheidend den Einfluss von Adrb2 auf die Knochenheilung moduliert.

NE induziert die Vegfa-Expression in Periostzellen durch den Adrb2-Signalweg

Da ein Mangel an Adrb2 bei ansonsten gesunden adulten Mäusen eine mangelnde Heilungsrate von Frakturen verursachte, könnte der Adrb2 ein wichtiger Regulator der Knochenheilung sein. Immhunhistochemische Untersuchungen von unbehandelten WT-Tieren zeigten, dass der Adrb2 sowohl in Osteoblasten als auch in Periostzellen des Femurs exprimiert wird. Um eine mechanistische Erklärung für die Rolle von Adrb2 bei der Förderung der Knochenheilung zu finden, wurden beide Zelltypen *in vitro* kultiviert. In Osteoblasten ergaben die Genexpressionsanalysen eine erhöhte Expression des Adrb2 im Vergleich zu anderen adrenergen Rezeptoren in diesen Zellen. In Periostzellen zeigte sich eine frühe, hohe Expression des Adrb2, welche im Verlauf der Zelldifferenzierung abnahm. Der beta1-adrenerge (Adrb1) und auch der beta3-adrenerge (Adrb3) Rezeptor zeigten hier ein unspezifisches und geringes Expressionsmuster. Die Behandlung der Zellen mit NE führte zu einer verringerten extrazellulären Mineralisierung der Osteoblasten, während die Osteogenese der Periostzellen unbeeinträchtigt blieb. Gleichermaßen zeigte die NE-Behandlung keinen Einfluss auf Knochenbildungsmarker in den Periostzellen. Da das Periost den gesamten Knochen umgibt und essenziell für die Vaskularisation ist, wurde die Expression neoangiogener Marker untersucht. Es wurde gezeigt, dass NE die Expression von Vegfa und dem Hypoxie-induzierten Faktor 1-alpha (Hif1a) auf mRNA-Ebene in Periostzellen aus WT-Tieren induzierte. Dies übersetzte sich auch in eine erhöhte Konzentration von

Vegfa im Überstand der Periostzellen. Ähnliche Effekte von NE zeigten sich auch in der Behandlung von Osteoblasten, was darauf hindeutet, dass Adrb2 eine Induktion der *Vegfa*- und *Hif1a*- Expression auch in anderen Zelltypen vermittelt.

Verstärkte NE-Adrb2-Signalübertragung induziert die Typ-H-Gefäßbildung während der Knochenheilung

Um die Rolle von Adrb2 in der Knochenheilung besser zu verstehen, wurden immunhistochemische Färbungen mit einem Adrb2-spezifischen Antikörper durchgeführt. Hier zeigte sich, dass Adrb2 neben Osteoblasten primär im Periost, der Knochenhaut, auf Proteinebene exprimiert wird. Das Periost ist nicht nur intensiv mit Nervenfasern innerviert, sondern trägt durch die Expression pro-angiogener Faktoren wie beispielsweise dem *Vegfa* auch entscheidend zur Vaskularisierung des heilenden Knochens bei. Daher wurde als nächstes die *Vegfa*-Expression im Skelett der adulten, 30 Wochen alten Tiere untersucht. Das intakte Skelett der *Adrb2*$^{-/-}$ Mäuse zeigte keine geänderte mRNA- und Proteinexpression von *Vegfa*. Dem Gegenüber wies das extrahierte Kallusgewebe der *Adrb2*$^{-/-}$ Gruppe drei Tage nach Femurosteotomie eine verringerte *Vegfa*-mRNA-Expression auf, welches an Tag 7 nicht mehr nachweisbar war. Weitere Analysen zum gleichen Zeitpunkt ergaben eine verminderte Vegfa-Konzentration im Serum der *Adrb2*$^{-/-}$ Mäuse. Diese Beobachtungen wurden durch immunhistochemische Färbungen bestätigt, bei denen die Vegfa-Signalintensität im Kallusgewebe von *Adrb2*$^{-/-}$ Tieren deutlich reduziert war. Frühere Studien belegen die zentrale Bedeutung von Vegfa für die Bildung von Typ-H-Gefäßen, die die Osteogenese an die Vaskularisation koppeln und durch die Koexpression von CD31 und Endomucin definiert sind [5,13]. Um dies für die Frakturheilung zu analysieren, wurde der Kallus am Ende der Vaskularisationsphase, am Tag 14 nach Femurosteotomie, immunhistochemisch auf das Vorliegen der Typ-H-Gefäße untersucht. Hier zeigten *Adrb2*$^{-/-}$ Mäuse eine Abnahme der Dichte an Typ-H-Gefäßen um bis zu 50 % im Vergleich zur WT-Gruppe. Zusammenfassend belegen diese Experimente, dass Adrb2 über die Expression von Vegfa die Bildung von Typ-H-Gefäßen im Kallus reguliert, was einen entscheidenden Einfluss auf die Knochenheilung hat.

Die pharmakologische Modulation der Adrb2-Signalübertragung steuert den Knochenumbau im intakten Skelett

Um diese Ergebnisse auf ihre translationale und therapeutische Relevanz hin zu überprüfen, wurde die pharmakologische Modulation des beta-adrenergen Systems in adulten WT-Tieren untersucht. Hierzu wurden der nicht-selektive Antagonist Propranolol (der sowohl Adrb1- als auch Adrb2-Rezeptoren blockiert) [14], der Adrb1-selektive Antagonist Atenolol [15] und der Adrb1-selektive Agonist Formoterol [16] verwendet. Im intakten Skelett der adulten Tiere führte die tägliche Injektion von Propranolol über drei

Wochen radiologisch zu einer Zunahme der trabekulären Knochenmasse in der Wirbelsäule und im distalen Oberschenkelknochen, was mittels µCT-Scan nachgewiesen wurde. Diese Ergebnisse wurden durch nicht-entkalkte Histologie der Lendenwirbelsäule bestätigt, bei der das Knochenvolumen in der Propranolol-Gruppe erhöht war. Die Behandlung mit Formoterol hingegen führte zu einer verringerten Anzahl von Trabekeln und einer erhöhten Trabekelseparation, wobei keine der Behandlungen Einfluss auf die Kortikalisdicke hatte. Dies wurde durch die Histologie der Lendenwirbelsäule bestätigt, bei der das Knochenvolumen in der Formoterol-Gruppe ebenfalls reduziert war. Der Adrb1-spezifische Antagonist Atenolol zeigte keinerlei Wirkung auf die Knochenmasse des intakten Skeletts.

Die pharmakologische Modulation der Adrb2-Signalübertragung steuert die Frakturheilung durch Bildung von Blutgefäßen im Kallus

Anschließend wurden die Auswirkungen von Propranolol, Formoterol und Atenolol auf die Knochenregeneration nach Femurosteotomie in adulten WT-Mäusen untersucht. Im Gegensatz zum intakten Skelett wurde mittels µCT-Scans festgestellt, dass die systemische Behandlung mit Propranolol über drei Wochen die Bildung neuen Knochens im Kallus reduzierte. Die systemische Behandlung mit Formoterol führte dagegen zu verbesserten radiologischen Ergebnissen. Bei der Behandlung mit Atenolol konnten keine Veränderungen bei der Knochenheilung beobachtet werden. Kryoschnitte des Frakturspaltes zeigten, dass die Propranolol-Behandlung zu einer geringeren Knochenbildung bei erhöhtem knorpeligem Anteil führte. Die Behandlung mit Formoterol hingegen erhöhte das mineralisierte Kallusvolumen. Auch die semiquantitative Auswertung der knöchernen Kallusüberbrückung zeigte eine hohe Rate an Pseudarthrosen in der Propranolol-Gruppe, wohingegen eine verbesserte Kallusüberbrückung bei Mäusen mit Formoterol-Behandlung beobachtet wurde. Als mögliche Erklärung für diese skelettalen Auswirkungen wurde schließlich die Dichte der Typ-H-Gefäße analysiert. Es konnte gezeigt werden, dass die Behandlung mit Propranolol zu einer verringerten Ausbildung von Typ-H-Gefäßen führte. Die Formoterol-Behandlung war mit einer Zunahme der Gefäßdichte im Kallus assoziiert. Atenolol zeigte hierbei keine Auswirkungen. Zusammenfassend zeigen diese Daten, dass ein pharmakologischer Adrb2-Antagonismus die Frakturheilung verschlechtert, wohingegen der Adrb2-Agonismus die Knochenregeneration verbessert.

1.3. Diskussion

Die vorliegenden Ergebnisse identifizieren erstmals eine entscheidende und altersabhängige Rolle des SNS und Adrb2 in der Frakturheilung. Es wurde gezeigt, dass trotz erhöhter Knochenmasse im nicht-frakturierten Skelett die Frakturheilung in adulten *Adrb2*$^{-/-}$ Mäusen erheblich verschlechtert ist. Mechanistisch wurde beobachtet, dass Adrb2 die Expression von *Vegfa* im Periost induziert, was zu einer gesteigerten Ausbildung osteogener Typ-H-Gefäße und einer verbesserten Kallusvaskularisation führt. Aus translationaler Perspektive resultierte die pharmakologische Hemmung von Adrb2 in einer verschlechterten Knochenheilung, während der Adrb2-Agonismus die Knochenregeneration verbesserte.

Bislang gab es nur wenige Studien bezüglich der Rolle des Adrb2-Signalweges in der Knochenregeneration, die zudem widersprüchliche Ergebnisse zur Funktion des SNS in der Frakturheilung beschrieben. Dies erscheint überraschend, da das SNS maßgeblich die Reaktionen des Körpers auf externen und internen Stress vermittelt. In diesem Zusammenhang beschrieb eine vorherige Studie, dass die Behandlung mit dem Adrb2-Antagonisten Propranolol die Frakturheilung bei Ratten nicht beeinflusst [17]. Über das Alter der Tiere wurde jedoch keine genaue Angabe gemacht. Eine andere Studie berichtete nach der Behandlung mit Propranolol über eine bessere Knochenheilung an einem unikortikalen Defekt in 12 Wochen jungen Ratten [18]. Es wurde auch beschrieben, dass die einmalige Injektion von Propranolol in 10 Wochen jungen Tieren die Knochenheilung in einem Modell für chronischen, psychosozialen Stress verbesserte [19]. Als Erklärung wurde hierbei eine Veränderung der Immunzellfunktion gefunden. Eine weitere Studie an 12 Wochen jungen Mäusen berichtete dagegen über eine höhere Kallusstabilität in der späten Phase der Knochenheilung nach dreiwöchiger Behandlung mit Reboxetin, einem selektiven NE-Wiederaufnahme-Inhibitor [20]. Auch die hier vorliegenden Ergebnisse der jungen Mäuse mit niedrigem Sympathikotonus lieferten keine klaren Erkenntnisse bezüglich der Rolle des Adrb2 in Knochenumbau oder Knochenregeneration. Erst adulte Tiere im Alter von 30 Wochen zeigten einen ausgeprägten Phänotyp in Bezug auf Knochenumbau und Knochenheilung. Als Ursache für diesen altersabhängigen Einfluss von Adrb2 auf das Skelettsystem konnte ein erhöhter NE-Gehalt in den Knochen adulter Mäuse nachgewiesen werden, der, wie bereits in anderen Studien beschrieben, durch eine verminderte lokale NE-Wiederaufnahme bedingt ist [21]. Diese Erkenntnis könnte erklären, wieso frühere Studien zur Rolle des SNS in der Frakturheilung an jüngeren Tieren unschlüssige oder gegenläufige Ergebnisse erbrachten. Diese Befunde stehen auch im Einklang mit einem insgesamt erhöhten Sympathikotonus bei adulten Tieren, was nicht nur in Tiermodellen, sondern auch beim Menschen nachgewiesen ist [12].

Adulte *Adrb2*$^{-/-}$ Mäuse weisen im nicht-frakturierten Skelett eine gesteigerte Knochenformation und eine verminderte Knochenresorption auf, wohingegen paradoxerweise eine stark beeinträchtigte Knochenheilung und eine hohe Rate an atrophen Pseudarthrosen beobachtet wird. Immunhistochemische Daten zeigten *in vivo*, dass der Adrb2 nicht nur auf Osteoblasten, sondern auch auf Periostzellen exprimiert wird. Als mechanistische Erklärung konnte in parallellaufenden *in vitro* Experimenten gezeigt werden, dass NE die Matrixmineralisierung in Periostzellen nicht beeinflusste, jedoch eine Adrb2-abhängige Induktion der pro-angiogenen Faktoren Vegfa und Hif1a bewirkt. Beide Mediatoren regulieren die Bildung von Typ-H-Blutgefäßen, die für die Knochenneubildung während der Frakturheilung unerlässlich sind [5,13]. Der Kallus der adulten *Adrb2*$^{-/-}$ Mäuse wies eine geringere Dichte an Typ-H-Gefäßen auf, was darauf hindeutet, dass die Interaktion von NE mit Adrb2 in Periostzellen ein entscheidender Regulator der Kallusvaskularisation ist. Die Tatsache, dass Vegfa in nicht-frakturierten Knochen von adulten *Adrb2*$^{-/-}$ Mäusen nicht reduziert war, deutet darauf hin, dass eine Verletzung für die Aktivierung der Adrb2-abhängigen Induktion von Vegfa im Skelett erforderlich ist. Klinisch führt eine Schädigung des Periosts, welches unter anderem mit einer hohen Dichte an Fasern des SNS innerviert wird, ebenfalls zu einer gestörten oder verlangsamten Knochenheilung [22]. Abschließend liefern die Daten der vorliegenden Studie auch eine Erklärung für die klinische Beobachtung, dass ältere Frakturpatienten eine niedrigere Rate an Pseudarthrosen aufweisen als junge Patienten mit geringerem Sympathikotonus [23–25].

Obwohl sich die vorliegende Studie in erster Linie auf die Rolle von Adrb2 im Periost konzentrierte, konnte in parallellaufenden *in vitro* Experimenten die Adrb2-abhängige Induktion von Vegfa auch in Osteoblasten nachgewiesen werden. Diese Daten deuten darauf hin, dass die NE-induzierte Signaltransduktion zur Produktion von pro-angiogenen Faktoren auch in anderen Zelltypen eine Rolle spielt. Bestätigt wird diese Beobachtung durch verschiedene Studien, die diese positive Regulation der Angiogenese in weiteren Geweben beschreiben. So ist zum Beispiel das infantile Haemangiom, der häufigste benigne Weichteiltumor im Kindesalter [26], durch eine überschießende Proliferation an Kapillargefäßen unklarer Ätiologie gekennzeichnet. Als Goldstandard in der Therapie wird derzeit die orale Behandlung mit Propranolol eingesetzt, welches zu einer Abnahme der Gefäßproliferation führt [27]. In ähnlicher Weise hat sich gezeigt, dass die adrenerge Signalübertragung über Adrb2 die Vegfa-abhängige Tumorvaskularisation in diversen weiteren Tumorentitäten fördert [28–30]. NE induzierte auch dosis- und zeitabhängig die *Vegfa*-Transkription in braunen Adipozyten, was ebenfalls durch Propranolol reversibel war [31,32]. Zusammengenommen zeigen diese Beobachtungen, dass NE in der Lage ist, Vegfa in einer Vielzahl verschiedener Zelltypen

zu induzieren, und im Falle der Knochenheilung zu einer allgemeinen Förderung der für die Osteogenese erforderlichen Typ-H-Gefäßbildung führt.

Der Einfluss von Adrb2 auf den Knochenumbau und die Knochenheilung wird nicht nur im adulten Organismus mit physiologisch gesteigertem Sympathikotonus ersichtlich, sondern zeigt sich auch bei Patienten mit einem Schädel-Hirn-Trauma (SHT). Betroffene Patienten weisen posttraumatisch einen Anstieg des Sympathikotonus mit erhöhten systemischen NE-Spiegeln auf [33–35]. Nach SHT kommt es nicht nur zu einem Knochenmasseverlust im nicht-frakturierten Skelett, sondern paradoxerweise auch zu einer deutlichen Verbesserung der Frakturheilung [36–38]. In Kooperation mit der Charité konnte in diesem Zusammenhang in parallellaufenden Experimenten gezeigt werden, dass der Einfluss auf den Knochenumbau und die Knochenregeneration eines SHT ebenfalls durch das SNS und den Adrb2 vermittelt wird. Mäuse mit einem experimentell induzierten SHT demonstrierten eine verbesserte Frakturheilung, die durch eine gesteigerte Expression von Vegfa und höhere Dichte an Typ-H-Gefäßen im Kallus erklärt werden konnte. Darüber hinaus war die gesteigerte Frakturheilung nach SHT in Adrb2-defizienten Mäusen aufgehoben. Schließlich war auch der SHT-induzierte Verlust an Knochenmasse im nicht-frakturierten Skelett in Adrb2-defizienten Mäusen nicht mehr zu beobachten. Zusammenfassend belegen diese Experimente, dass die Auswirkungen eines SHT im frakturierten und nicht-frakturierten Skelett über Adrb2 vermittelt werden.

Die vorliegenden Daten identifizierten somit den Zelloberflächenrezeptor Adrb2 als neuartiges Zielprotein für die Regulation der Knochenheilung. Da es derzeit klinisch keine pharmakologischen Optionen gibt, die die Knochenheilung zuverlässig verbessern [4,8], wurde die medikamentöse Modulation von Adrb2 und deren Auswirkung auf die Knochenregeneration untersucht. Zunächst wurden adulte WT-Mäuse mit dem selektiven Adrb2-Agonisten Formoterol ab dem Zeitpunkt der Osteotomie behandelt. Die systemische Anwendung dieses Medikaments, das klinisch häufig als Inhalationspräparat bei Asthma und chronisch obstruktiver Lungenerkrankung eingesetzt wird, förderte die Bildung von Typ-H-Gefäßen und verbesserte die Frakturheilung. Dies zeigt, dass pharmakologischer Adrb2-Agonismus, zumindest bei Mäusen, einen geeigneten Ansatz zur Stimulierung der Knochenregeneration darstellt. Da die klinische Anwendung mittels Inhalation-Präparaten auch zu einem nachweislichen Anstieg von Formoterol im Plasma bereits fünf Minuten nach Applikation führt [39], könnten bereits retrospektive Studien wichtige Erkenntnisse zu einem möglichen Effekt auf die Knochenheilung und den Knochenumbau liefern. Ebenso könnte die topische Applikation von Formoterol oder anderen Adrb2-Agonisten in den Frakturspalt, z. B. durch künstliche Matrizen oder Scaffolds, eine geeignete Option zur Verbesserung der Frakturheilung bei Patienten mit erhöhtem Pseudarthroserisiko darstellen.

Zusätzlich deuten die erhobenen Daten auch darauf hin, dass eine Adrb2-Blockade zu einer beeinträchtigten Frakturheilung führen könnte. Hier konnte beobachtet werden, dass der nicht-selektive Betablocker Propranolol bei adulten Mäusen eine verzögerte Frakturheilung verursacht, indem er die Neovaskularisation des Kallus beeinträchtigt. Dies ist von hoher klinischer Relevanz, da die Häufigkeit altersbedingter Frakturen stetig zunimmt [7] und fast jeder fünfte Mensch im Alter von über 60 Jahren täglich Betablocker einnimmt [40]. Diese Ergebnisse werden durch eine kürzlich durchgeführte, unabhängige Studie gestützt, in der die Einnahme von Betablockern bei 253.266 Patienten nach Kontrolle von Geschlecht, Alter und Komorbidität mit einem um 13 % erhöhten Risiko einer Pseudarthrose verbunden war [41]. Es ist daher sinnvoll, die Auswirkungen dieser Medikamentenklasse auf die Frakturheilung beim Menschen weiter zu untersuchen und zu prüfen, ob eine Unterbrechung der Betablocker-Therapie bei Frakturpatienten, solange dies aus kardiovaskulärer Sicht vertretbar ist, gerechtfertigt ist.

Die vorliegende Studie hat mehrere Einschränkungen. Zum einen wurde primär ein globales Adrb2-Defizienzmodell verwendet. Obwohl dies die Gesamtschlussfolgerungen nicht beeinträchtigt, sind für den genauen Mechanismus Folgeexperimente an Mäusen mit konditionaler Deletion von Adrb2 in Periostzellen, Osteoblasten oder anderen Zelltypen erforderlich. Zudem könnten auf Grund der Gruppengrößen (n= 6- 9) subtile Veränderungen von jungen *Adrb2*$^{-/-}$ Mäusen möglicherweise nicht erfasst worden sein. Schließlich sollten prospektive klinische Studien durchgeführt werden, um beispielsweise zu untersuchen, ob der Einsatz von Betablockern mit schlechteren Ergebnissen bei der Knochenheilung verbunden ist. Die hier beschriebenen Daten an frakturierten Mäuseknochen und vorherige Beobachtungen anderer Wissenschaftler und Wissenschaftlerinnen am nicht-frakturierten Knochen [42,43], deuten insgesamt darauf hin, dass Adrb2 hauptsächlich die Wirkungen von NE auf das Skelett der Mäuse vermittelt. Im Gegensatz dazu gibt es mittlerweile klinische Evidenz, dass in Menschen nicht Adrb2, sondern primär Adrb1 an der Regulation des Knochenumbaus involviert ist [44]. Obwohl der Adrb1-Antagonist Atenolol in der vorliegenden Arbeit keinen Einfluss auf die Frakturheilung bei adulten Mäusen hatte, sind weitere Studien notwendig, um die Rolle von Adrb1 und Adrb2 bei der Frakturheilung des Menschen zu differenzieren und mögliche therapeutische Nutzen zu überprüfen.

SCIENCE TRANSLATIONAL MEDICINE | RESEARCH ARTICLE

BONE DISEASE

Increased β_2-adrenergic signaling promotes fracture healing through callus neovascularization in mice

Denise Jahn[1,2]†, Paul Richard Knapstein[3]†, Ellen Otto[1,2]†, Paul Köhli[1,2,4]†, Jan Sevecke[3], Frank Graef[1,4], Christine Graffmann[2], Melanie Fuchs[1,2], Shan Jiang[3], Mayla Rickert[3], Cordula Erdmann[3], Jessika Appelt[1,2], Lawik Revend[1], Quin Küttner[1], Jason Witte[2], Adibeh Rahmani[1,2], Georg Duda[2], Weixin Xie[3], Antonia Donat[3], Thorsten Schinke[5], Andranik Ivanov[6,7], Mireille Ngokingha Tchouto[6], Dieter Beule[6,7], Karl-Heinz Frosch[3], Anke Baranowsky[3], Serafeim Tsitsilonis[1,2]*, Johannes Keller[3]*

Traumatic brain injury (TBI) leads to skeletal changes, including bone loss in the unfractured skeleton, and paradoxically accelerates healing of bone fractures; however, the mechanisms remain unclear. TBI is associated with a hyperadrenergic state characterized by increased norepinephrine release. Here, we identified the β_2-adrenergic receptor (ADRB2) as a mediator of skeletal changes in response to increased norepinephrine. In a murine model of femoral osteotomy combined with cortical impact brain injury, TBI was associated with ADRB2-dependent enhanced fracture healing compared with osteotomy alone. In the unfractured 12-week-old mouse skeleton, ADRB2 was required for TBI-induced decrease in bone formation and increased bone resorption. Adult 30-week-old mice had higher bone concentrations of norepinephrine, and ADRB2 expression was associated with decreased bone volume in the unfractured skeleton and better fracture healing in the injured skeleton. Norepinephrine stimulated expression of vascular endothelial growth factor A and calcitonin gene–related peptide-α (αCGRP) in periosteal cells through ADRB2, promoting formation of osteogenic type-H vessels in the fracture callus. Both ADRB2 and αCGRP were required for the beneficial effect of TBI on bone repair. Adult mice deficient in ADRB2 without TBI developed fracture nonunion despite high bone formation in uninjured bone. Blocking ADRB2 with propranolol impaired fracture healing in mice, whereas the ADRB2 agonist formoterol promoted fracture healing by regulating callus neovascularization. A retrospective cohort analysis of 72 patients with long bone fractures indicated improved callus formation in 36 patients treated with intravenous norepinephrine. These findings suggest that ADRB2 is a potential therapeutic target for promoting bone healing.

INTRODUCTION

Bone remodeling and fracture healing are essential survival functions that are evolutionarily conserved across a wide range of species. Because of increased life expectancy of the general population, we are now faced with a high incidence of skeletal disorders, such as osteoporosis and age-related fractures (*1*, *2*). Fractures treated according to best practice are still associated with a 10 to 15% risk of bone failure to heal, resulting in nonunion (*3*). Impaired fracture healing places a heavy burden on patients, often requiring multiple revision surgeries and predisposing them to further complications, resulting in prolonged immobilization, disability, or even death (*4*). Despite extensive research over past decades, no pharmacologic agent is clinically available that reproducibly improves fracture healing and reduces the incidence of fracture nonunion with an acceptable safety profile (*5*).

Bone remodeling and regeneration are accomplished by the coordinated activity of osteoblasts and osteoclasts, which are regulated not only by local cytokines and growth factors but also by systemic hormones and neurotransmitters (*3*). Fracture healing is also dependent on the integrity and function of the periosteum, which circumferentially covers the bone and promotes callus neovascularization with osteogenic type-H vessels after bone injury (*6*). The sympathetic nervous system and its major effector molecule, norepinephrine (NE), have been identified as potent regulators of skeletal health through inhibiting bone formation and promoting bone resorption (*7, 8*).

The clinical observation that traumatic brain injury (TBI) is associated with improved fracture healing is of paramount importance from both a clinical and basic science perspective. Although TBI ultimately results in a reduction in bone density and bone quality of the unfractured skeleton (*9*–*11*), regeneration of fractured bone is paradoxically increased with TBI (*12*). A thorough pathophysiological understanding of the underlying mechanism is still lacking (*11, 12*) because trauma to the central nervous system results in multiple and complex biological changes in the organism. TBI is clinically associated with endocrine abnormalities and a hyperadrenergic state with elevated plasma catecholamine concentrations (*13, 14*). The latter is thought to reflect a generalized stress response to trauma to restore vital homeostasis in the face of TBI because activation of the sympathetic nervous system results in increased secretion of catecholamines, including NE, to the periphery (*15*). In this context, NE is elevated in a dose-dependent manner according to the severity of the injury (*16*). In addition to a hyperadrenergic state, increased serum

[1]Charité—Universitätsmedizin Berlin, corporate member of Freie Universität Berlin and Humboldt-Universität zu Berlin, Center for Musculoskeletal Surgery, 13353 Berlin, Germany. [2]Berlin Institute of Health at Charité—Universitätsmedizin Berlin, Julius Wolff Institute, 13353 Berlin, Germany. [3]University Medical Center Hamburg-Eppendorf, Department of Trauma and Orthopedic Surgery, 20251 Hamburg, Germany. [4]Berlin Institute of Health at Charité—Universitätsmedizin Berlin, BIH Biomedical Innovation Academy, BIH Charité Junior Clinician Scientist Program, 13353 Berlin, Germany. [5]University Medical Center Hamburg-Eppendorf, Department of Osteology and Biomechanics, 20251 Hamburg, Germany. [6]Berlin Institute of Health at Charité—Universitätsmedizin Berlin, Core Unit Bioinformatics, 10117 Berlin, Germany. [7]Max-Delbrück-Center for Molecular Medicine, 13125 Berlin, Germany.
*Corresponding author. Email: serafeim.tsitsilonis@charite.de (S.T.); j.keller@uke.de (J.K.)
†These authors contributed equally to this work.

concentrations of neurotransmitters are present after TBI, some of which are known to affect bone remodeling and fracture healing, including calcitonin gene–related peptide (CGRP) (*17*–*19*). However, the impact of CGRP on the skeletal manifestations in patients with TBI remains unclear.

Using our previously reported mouse model combining femoral fracture with standardized TBI (*20*), we show here that TBI affects both systemic bone remodeling and fracture healing through the β_2-adrenergic receptor (ADRB2). After TBI in mice, increased NE concentrations reduce bone formation and promote bone resorption in the unfractured skeleton in an ADRB2-dependent manner. During bone fracture healing after TBI, increased NE-ADRB2 signaling induces the expression of vascular endothelial growth factor A (VEGFA) in periosteal cells and osteoblasts, resulting in increased formation of osteogenic type-H vessels and improved vascularization of the fracture callus. Although ADRB2 plays only a minor role in bone healing in otherwise healthy and young mice, it substantially promoted bone regeneration in adult mice with physiologically increased sympathetic tone.

RESULTS

Accelerated bone fracture healing after TBI is associated with enhanced callus remodeling in mice

To delineate the impact of TBI on bone regeneration, we first used our mouse model combining a controlled cortical TBI with a fracture model of femoral osteotomy stabilized by an external fixator (*20*). Consistent with our prior results, microcomputed tomography (μCT) scanning showed increased bone and tissue volume of the fracture callus of 12-week-old mice with combined TBI and fracture 14 days after injury (Fig. 1A). This finding was confirmed by Movat Pentachrome histological staining on undecalcified callus sections, where an increased mineralized callus area and cartilage area were observed (Fig. 1B). Cellular histomorphometry showed an increase in both osteoclast (Fig. 1C) and osteoblast parameters in the callus of mice with TBI compared with fracture alone (Fig. 1D). Assessment of the calcein-labeled area in the fracture callus demonstrated that TBI increased the formation of newly formed bone in the fracture gap (Fig. 1E).

TBI-induced high sympathetic tone is associated with impaired bone formation in the unfractured skeleton

In 12-week-old mice, histological analysis of unfractured bone sections 14 days after TBI revealed decreased bone mass in the spine compared with sham animals, which was accompanied by a reduction in trabecular thickness (Fig. 2A). Similar results were obtained using μCT scanning of the lumbar spine, which also demonstrated a reduced trabecular bone mass and trabecular thickness (fig. S1A). Histomorphometric quantification of bone cells showed increased osteoclast number and surface area (Fig. 2B), whereas osteoblast number and surface area were decreased (Fig. 2C). In the midshaft area of the femur, cortical thickness was unaltered by TBI (fig. S1B); however, TBI led to decreased biomechanical stability as measured using a three-point bending test (fig. S1C). In the distal femur, trabecular bone volume was also reduced, explained by reduced trabecular number and thickness (Fig. 2D). RNA sequencing (RNA-seq) of the unfractured distal femur including the bone marrow revealed decreased expression of genes encoding osteoblast markers 3 days after TBI, including alkaline phosphatase (*Alpl*), osterix (*Sp7*), bone sialoprotein (*Ibsp*), bone gamma-carboxyglutamate protein (*Bglap*), phosphate-regulating endopeptidase X-linked (*Phex*), and periostin (*Postn*), whereas osteoclast markers were not affected (Fig. 2E). Subsequent quantitative reverse transcription polymerase chain reaction (qRT-PCR) confirmed that TBI resulted in decreased expression of osteoblast marker genes in the unfractured femur, whereas

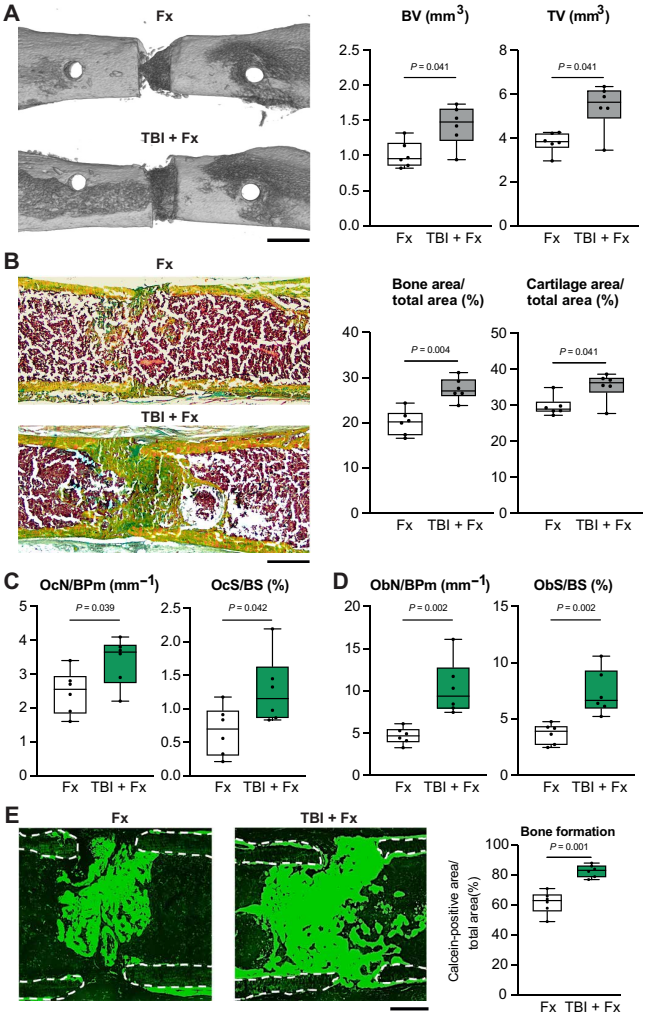

Fig. 1. TBI improves fracture healing in mice through enhanced callus remodeling. (**A**) Representative μCT images of the fractured femora 14 days after fracture only (Fx) or combined injury (TBI + Fx) in 12-week-old WT mice, with quantification of bone volume (BV) and tissue volume (TV) in the callus. Scale bar, 2 mm. (**B**) Representative callus sections of femora from the same mice stained with Movat Pentachrome (yellow, mineralized bone; green, cartilage; red, bone marrow) and histomorphometric quantification of bone area and cartilage area per total area. Scale bar, 500 μm. (**C**) Quantification of osteoclast numbers per bone perimeter (OcN/BPm) and percent osteoclast surface per bone surface (OcS/BS). (**D**) Quantification of osteoblast numbers per bone perimeter (ObN/BPm) and percent osteoblast surface per bone surface (ObS/BS). (**E**) Representative fluorescence images of calcein labeling (green) in the fracture gap indicative of newly formed bone. Dotted white lines show the fracture ends. Scale bar, 300 μm. Quantification of calcein-positive area per total area as a marker of bone formation in the callus. For all panels, $n = 6$ mice per group, data are presented as box plots with median and 25th and 75th quantiles, and whiskers indicate upper and lower extremes. Data were analyzed by Mann-Whitney *U* test (A and B) or two-tailed Student's *t* test (C to E).

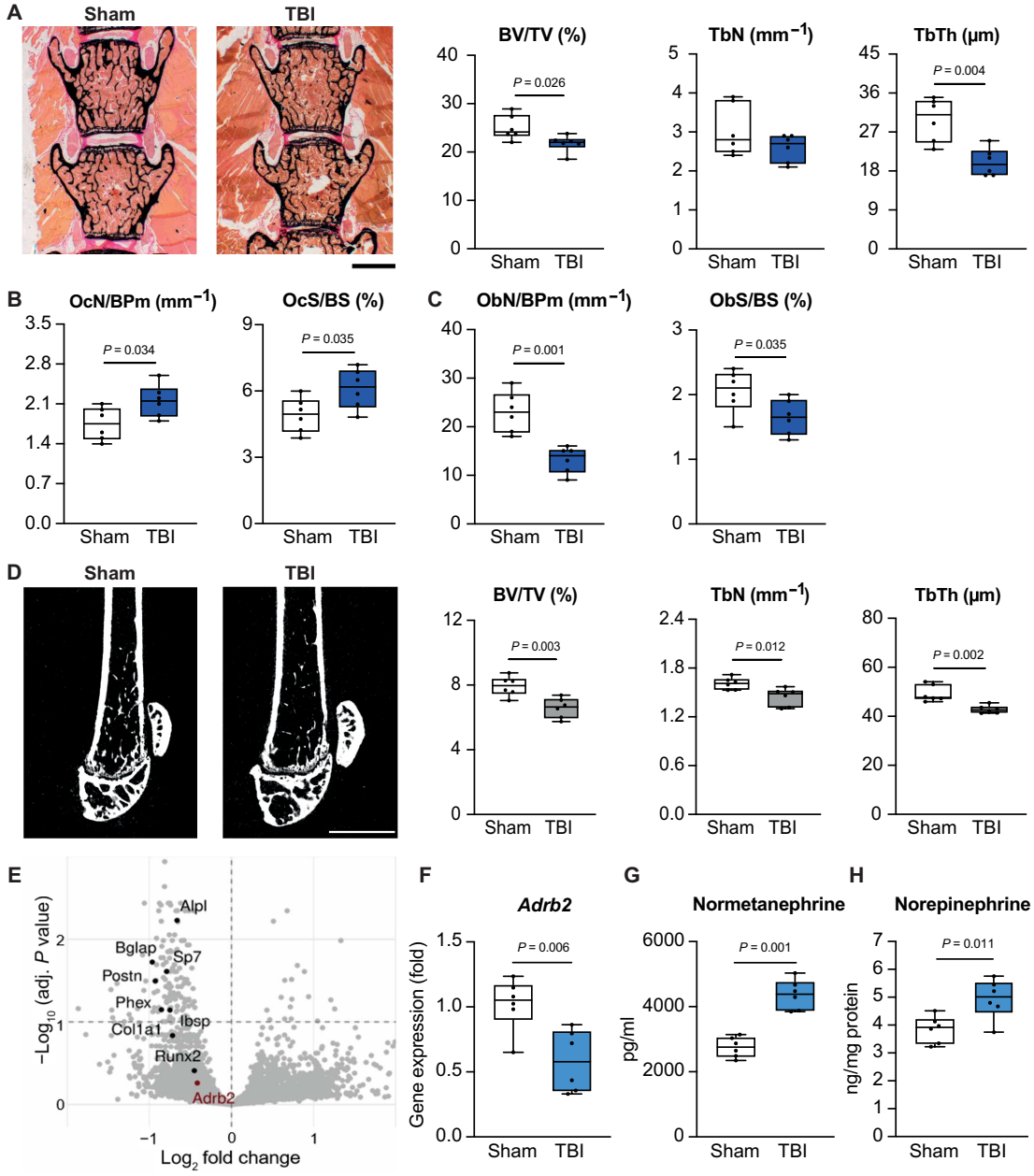

Fig. 2. TBI causes systemic bone loss in the unfractured mouse skeleton. (**A**) Von Kossa and Van Gieson staining of undecalcified vertebra sections (L3 and L4) was performed 14 days after sham operation or TBI in 12-week-old WT mice. Static histomorphometry of BV/TV, trabecular number (TbN), and trabecular thickness (TbTh) was performed. Scale bar, 500 μm. (**B**) Quantification of OcN/BPm and OcS/BS. (**C**) Quantification of ObN/BPm and ObS/BS. (**D**) Representative μCT images of the distal femora of the same groups and quantification of structural parameters of bone volume, trabecular number, and trabecular thickness. Scale bar, 2 mm. (**E**) Volcano plot of the RNA-seq results of the unflushed distal femora of mice 3 days after sham operation ($n = 3$ mice) or TBI ($n = 4$ mice). The *x* axis represents the relative gene expression changes, and the *y* axis shows the adjusted *P* value transformed in $-\log_{10}$ scale. (**F**) Expression of *Adrb2* measured by qRT-PCR in the distal femora of an independent set of 12-week-old WT mice 3 days after TBI injury relative to sham controls. (**G**) Serum concentration of normetanephrine 3 days after surgery in the same mice. (**H**) NE content in the flushed femora of the same groups. In (A) to (D) and (F) to (H), $n = 6$ mice per group, data are presented as box plots with median and 25th and 75th quantiles, and whiskers indicate extremes. Data were analyzed by Mann-Whitney *U* test (A) or two-tailed Student's *t* test (B to D and F to H).

expression of osteoclast markers was not altered (fig. S1, D and E). Together, these analyses indicated that TBI negatively affects bone volume by decreasing bone formation and increasing bone resorption in the unfractured skeleton.

RNA-seq data also showed reduced expression of *Adrb2* after TBI ($P = 0.037$; adjusted $P = 0.550$). ADRB2 was previously identified to inhibit bone formation by osteoblasts and stimulate osteoclastogenesis (*21*). ADRB2 is down-regulated upon overstimulation by its endogenous ligand NE (*22*). The down-regulation of *Adrb2* in the femur of wild-type (WT) TBI mice was confirmed in an independent cohort of WT mice with TBI by qRT-PCR (Fig. 2F). Subsequent measurement of the stable NE metabolite normetanephrine showed elevated serum concentrations of this metabolite 3 days after TBI (Fig. 2G). Likewise, NE content in the femora of mice with TBI was increased, supporting previous reports of a hyperadrenergic state in patients with TBI (Fig. 2H) (*23*–*28*).

The skeletal effects of TBI on the unfractured and fractured skeleton are abrogated in *Adrb2*$^{-/-}$ mice

In the distal femur of untreated 12-week-old WT mice, immunohistochemistry with an ADRB2-specific antibody showed strong signal intensity in osteoblasts lining trabecular bone and intense staining in the periosteum, which is a pivotal tissue for fracture repair (Fig. 3A). *Adrb2* gene expression in whole callus tissue was elevated during the fracture healing process in WT mice after osteotomy, which was supported by immunohistochemistry demonstrating increasing ADRB2 signal intensity during fracture healing (Fig. 3, B and C). To test the functional role of ADRB2, we next subjected 12-week-old *Adrb2*$^{-/-}$ mice to TBI with or without a femoral osteotomy and assessed fracture healing and bone remodeling. In the fractured skeleton of *Adrb2*$^{-/-}$ mice, μCT scanning demonstrated that TBI had no effect on bone healing in the absence of ADRB2 (Fig. 3D). This finding was confirmed in undecalcified callus sections of *Adrb2*$^{-/-}$ mice stained with Movat Pentachrome, where no alterations in mineralized bone or cartilage area in the callus were observed after TBI in the absence of ADRB2 (Fig. 3E). Similar observations were made in the unfractured skeleton of mice with TBI or sham operation only. In *Adrb2*$^{-/-}$ mice, bone volume and structure in the spine remained unaltered 14 days after TBI (Fig. 3, F and G). Histologically, osteoclast and osteoblast parameters were also unchanged in 12-week-old *Adrb2*$^{-/-}$ mice with TBI compared with sham controls (Fig. 3H). Likewise, no effect of TBI on bone architecture was found in the spine or femora of *Adrb2*$^{-/-}$ mice using μCT scanning (fig. S2, A and B). The biomechanical stability of the unfractured femora was unaltered (fig. S2C), and *Adrb2*$^{-/-}$ mice had normal expression of osteoclast and osteoblast parameters in the femoral midshaft (fig. S2, D and E).

Adult *Adrb2*$^{-/-}$ mice display impaired bone healing

Whereas the inhibitory impact of ADRB2 on bone formation by osteoblasts and its pro-resorptive effect on osteoclasts are well established (*29*), a beneficial role of ADRB2 in fracture repair has been understudied. Thus, we next analyzed bone remodeling and repair in 12-week-old *Adrb2*$^{-/-}$ mice. Undecalcified histology of the spine showed no alteration in bone architecture or cellular remodeling in *Adrb2*$^{-/-}$ mice at this age (Fig. 4A). Likewise, μCT scanning of the distal femur showed no differences between *Adrb2*$^{-/-}$ mice and WT littermates (fig. S3A). Healing outcomes 7, 14, and 21 days after osteotomy were not altered in *Adrb2*$^{-/-}$ mice (Fig. 4, B to D, and fig. S3, B and C). In contrast, *Adrb2*$^{-/-}$ mice at the age of 30 weeks (hereafter referred to as adult) had increased trabecular bone mass in the spine, which was explained by elevated indices of bone formation and reduced osteoclast parameters (Fig. 4E). Similar observations were made in the distal femur, which displayed increased bone volume and trabecular number (fig. S4A). Assessing fracture in 30-week-old adult mice both radiologically and histologically, *Adrb2*$^{-/-}$ mice exhibited a higher cartilage area at day 7 and impaired callus mineralization and maturation at 14 days after osteotomy (fig. S4, B and C). At 21 days after osteotomy, ADRB2 deficiency resulted in insufficient bone formation in the fracture callus, with excessive cartilage content and high rates of fracture nonunion (Fig. 4, F to H). Tartrate-resistant acid phosphatase (TRAP) activity staining showed a decrease in osteoclast parameters in the callus of adult *Adrb2*$^{-/-}$ mice 21 days after fracture (Fig. 4I). Moreover, osteoblast numbers and osteoblast surface area were also reduced in adult mutant animals, accompanied by a reduction in the formation of new bone as evidenced by visualization of calcein incorporation into the healing bone at this time point (Fig. 4J). The data suggest that in adult mice ADRB2 deficiency results in high bone mass in the unfractured skeleton and impaired fracture healing. Sympathetic tone and production of NE is known to progressively increase with age (*30*). Serum normetanephrine concentrations did not differ between young (12-week-old) and adult (30-week-old) WT mice; however, the expression of *Slc6a2*, which mediates the reuptake of NE into bone cells and thus controls extracellular NE concentrations in the skeleton, was reduced in adult mice (fig. S5, A and B), in line with previous reports (*31*). This lower gene expression in adult bone was associated with an increased femur NE content compared with 12-week-old young animals, suggesting enhanced adrenergic signaling in the skeleton of adult animals (fig. S5C).

NE directly induces VEGFA expression in periosteal cells through ADRB2

Deficiency of ADRB2 blunted the impact of TBI on bone regeneration and caused fracture nonunion in otherwise healthy adult mice; thus, ADRB2 may be a regulator of bone healing in conditions of increased adrenergic signaling. ADRB2 was expressed in both osteoblasts and periosteal cells in the femur; therefore, we next assessed *Adrb2* expression in these two cell types in vitro. In cultured osteoblasts from 12- to 14-week-old WT mice, *Adrb2* was increased during in vitro osteogenic differentiation, whereas there was comparably lower expression of β_1 and β_3 adrenoreceptors (*Adrb1* and *Adrb3*, respectively) (Fig. 5A). Periosteal cells showed a high expression of *Adrb2* at early stages of differentiation, which declined later during cell differentiation (Fig. 5B). In contrast, *Adrb1* showed a nonspecific and low expression pattern during periosteal cell differentiation, and *Adrb3* was barely expressed in these cell cultures. Next, continuous supplementation of osteogenic culture medium with NE resulted in a decreased extracellular matrix mineralization in osteoblasts, whereas osteogenesis in periosteal cells was not affected (Fig. 5C). In line with this finding, NE did not alter the expression of bone formation markers in periosteal cells, independent of whether periosteal cells were derived from calvariae or femur bones (Fig. 5D and fig. S6A). Because the periosteum is required for bone vascularization (*32*), a prerequisite for fracture healing, we next monitored the expression of neo-angiogenic markers. We found that NE robustly induced the expression of *Vegfa* and hypoxia-inducible factor 1α (*Hif1a*) in WT but not *Adrb2*$^{-/-}$ periosteal

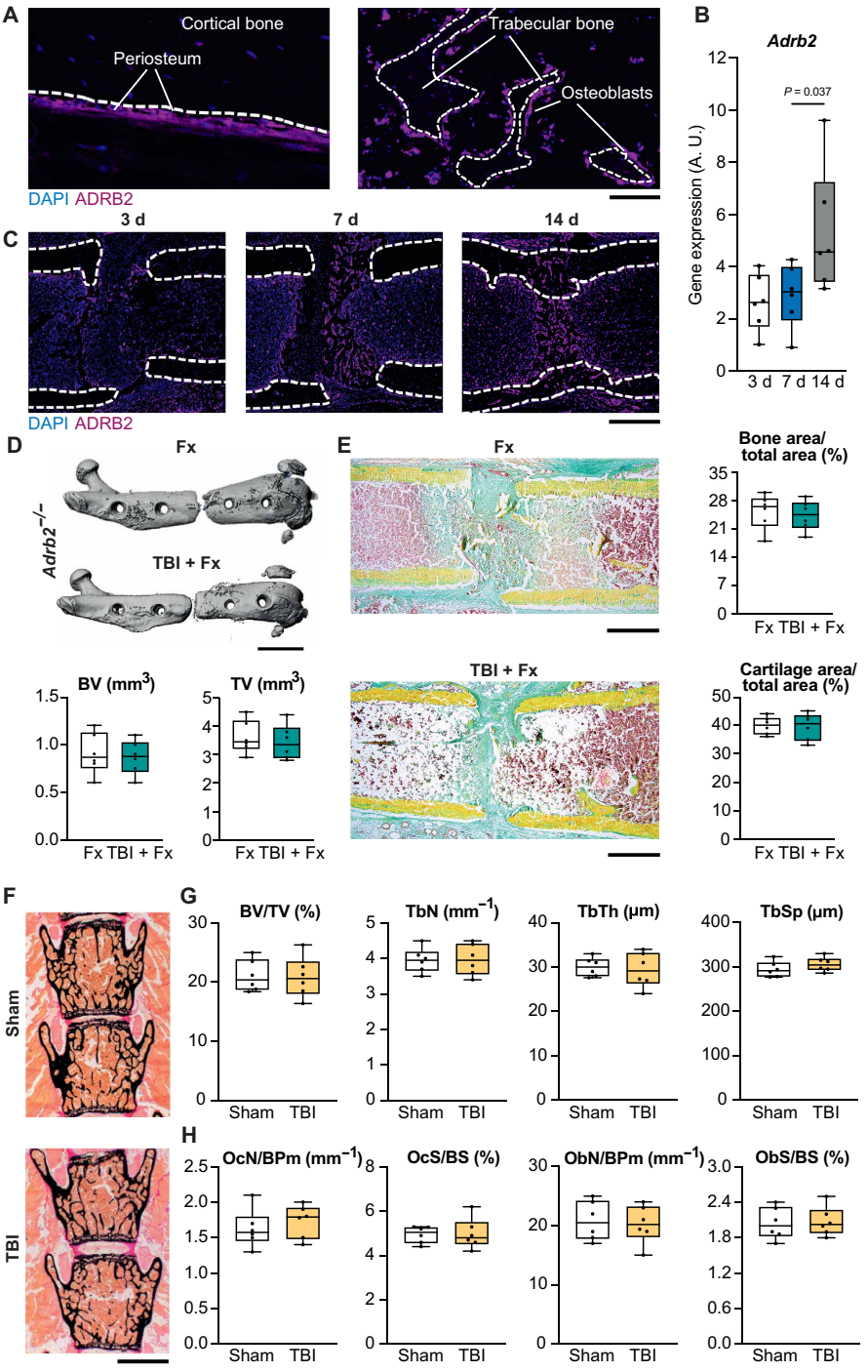

Fig. 3. ADRB2 deficiency prevents the skeletal effects of TBI on bone remodeling and regeneration. (**A**) Representative immunohistochemistry for ADRB2 in the trabecular and cortical bone of the distal femur of 12-week-old uninjured WT mice. Scale bar, 50 µm. (**B**) Gene expression analysis by qRT-PCR of *Adrb2* in the callus at the indicated time points after fracture in 12-week-old WT mice. A.U., arbitrary copy number units per housekeeping gene. (**C**) Representative ADRB2 immunohistochemical staining of callus sections derived from 12-week-old WT mice at the indicated time points after osteotomy. Dotted white lines indicate the facture ends. Scale bar, 400 µm. (**D**) Representative µCT images of the fractured femora 21 days after fracture only (Fx) or combined injury (TBI + Fx) in 12-week-old *Adrb2*$^{-/-}$ mice and quantification of callus BV and TV. Scale bar, 3 mm. (**E**) Representative callus Movat Pentachrome staining of Fx and TBI + Fx mice 21 days after surgery (yellow, mineralized bone; green, cartilage; red, bone marrow) and histomorphometric quantification of bone area per total area and cartilage area per total area in the same mice. Scale bar, 400 µm. (**F**) Von Kossa and Van Gieson staining of undecalcified vertebra sections (L3 and L4) 14 days after sham operation or TBI. Scale bar, 500 µm. (**G**) Static histomorphometry of BV/TV, TbN, TbTh, and TbSp (12-week-old *Adrb2*$^{-/-}$ mice). (**H**) Quantification of OcN/BPm, OcS/BS, ObN/BPm, and ObS/BS in the same mice. For (A) to (H), $n = 6$ mice per group, all numerical data are presented as box plots with median and 25th and 75th quantiles, and whiskers indicate extremes. For (B), data were analyzed by one-way ANOVA and Tukey's post hoc test. For (D), (E), (G), and (H), data were analyzed by two-tailed Student's *t* test.

cells (Fig. 5E and fig. S6B). This effect was not only detectable at the mRNA level but also translated into increased concentrations of VEGFA in the supernatant of periosteal cells (Fig. 5F). NE also induced the expression of *Vegfa* and *Hif1a* in bone marrow–derived osteoblasts, demonstrating that ADRB2 mediates *Vegfa* and *Hif1a* induction also in cell types other than periosteal cells (fig. S6C).

Enhanced NE-ADRB2 signaling controls type-H vessel formation during bone healing

To test the implications of these results in vivo, we next evaluated VEGFA expression in unfractured and fractured femora of *Adrb2*$^{-/-}$ mice at the age of 30 weeks. VEGFA mRNA and protein expression was not altered in the unfractured bones from naïve *Adrb2*$^{-/-}$ mice (fig. S7, A and B). However, gene expression analysis of extracted

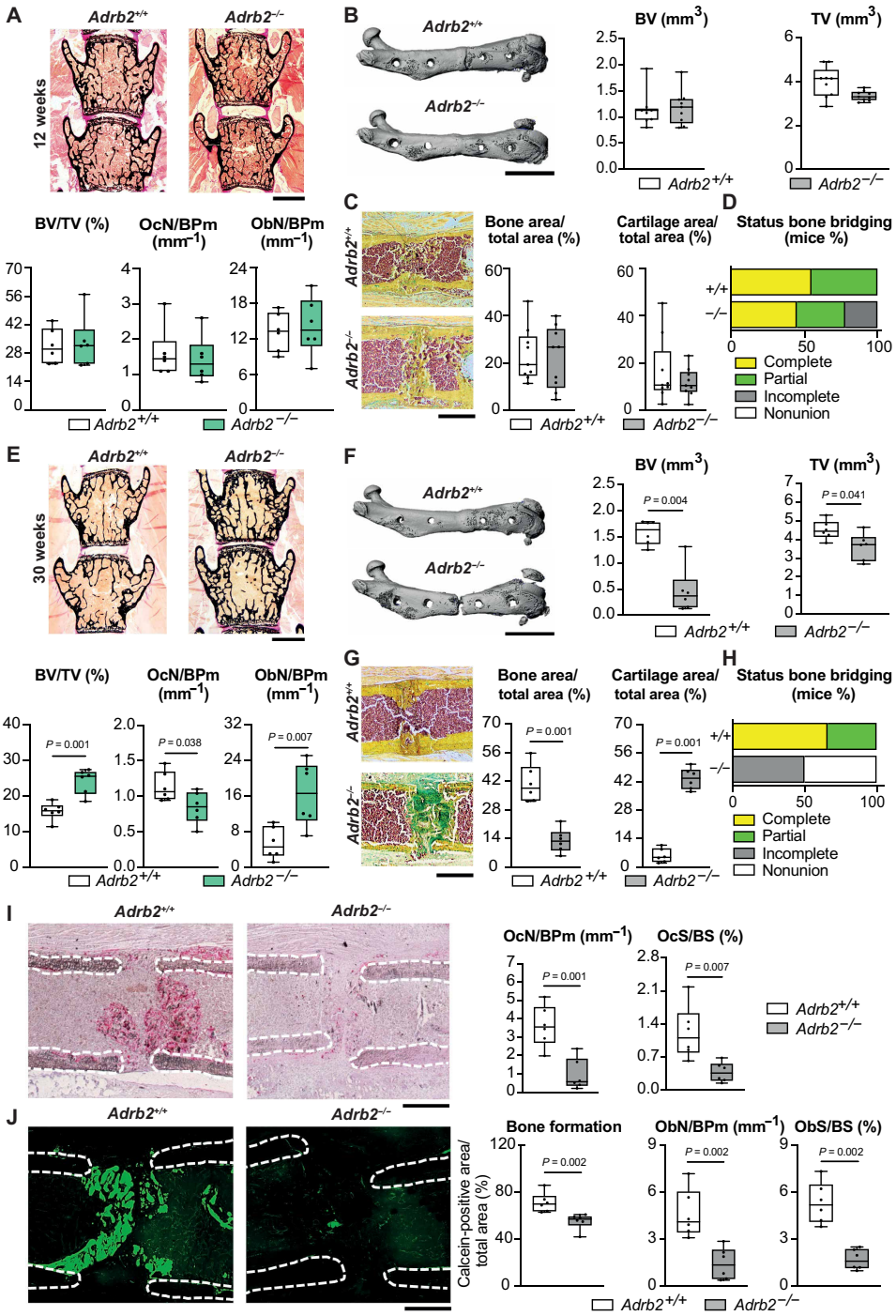

Fig. 4. ADRB2 plays an age-dependent role in fracture healing. (**A** to **D**) Evaluation of bone remodeling and bone regeneration in 12-week-old *Adrb2*$^{+/+}$ and *Adrb2*$^{-/-}$ mice. (A) Von Kossa and Van Gieson staining of undecalcified vertebra sections (L3 and L4) and histomorphometry of BV/TV, OcN/BPm, and ObN/BPm in uninjured mice (n = 6 mice per group). Scale bar, 500 μm. (B) Representative μCT images of the fractured femora in 12-week-old mice 21 days after fracture and quantification of callus BV and TV (n = 9 mice per group). Scale bar, 4 mm. (C) Representative callus sections stained with Movat Pentachrome in the same mice and quantification of bone area per total area and cartilage area per total area (n = 9 mice per group). Scale bar, 500 μm. (D) Semiquantitative evaluation of osseous callus bridging in the same mice. (**E** to **J**) Evaluation of bone remodeling and bone regeneration in 30-week-old *Adrb2*$^{+/+}$ and *Adrb2*$^{-/-}$ mice (n = 6 mice per group). (E) Von Kossa and Van Gieson staining of undecalcified vertebra sections (L3 and L4) and histomorphometry of BV/TV, OcN/BPm, and ObN/BPm in uninjured mice. Scale bar, 500 μm. (F) Representative μCT images of the fractured femora in 30-week-old adult mice of the indicated genotypes 21 days after fracture and quantification of callus BV and TV. Scale bar, 4 mm. (G) Representative callus sections stained with Movat Pentachrome in the same mice and quantification of bone area per total area and cartilage area per total area. Scale bar, 500 μm. (H) Semiquantitative evaluation of osseous callus bridging in the same mice. (I) Representative TRAP-stained (red) callus sections in 30-week-old mice of the indicated genotypes and quantification of OcN/BPm and OcS/BS. Scale bar, 400 μm. (J) Representative fluorescent images of calcein labeling (green) in the callus and quantification of calcein-positive area per total area, ObN/BPm, and ObS/BS in the same mice. Scale bar, 300 μm. For (I) and (J), dotted white lines show the fracture ends. All data are presented as box plots with median and 25th and 75th quantiles, and whiskers indicate extremes with the exception of (D) and (H). Data were analyzed by two-tailed Student's t test (A, E, G, and I) or Mann-Whitney U test (B, C, F, and J).

whole callus tissue showed reduced *Vegfa* mRNA expression in *Adrb2*$^{-/-}$ mice compared with WT littermates during the very early phase of bone regeneration, 3 days after surgery, but not at day 7 (Fig. 6A). This resulted in decreased serum VEGFA concentrations during fracture healing 3 days after osteotomy (Fig. 6B). Immunohistochemistry of undecalcified cryosections of the fracture callus at day 3 confirmed reduced VEGFA expression in the callus of *Adrb2*$^{-/-}$ mice (Fig. 6C and fig. S8A). In the callus of WT mice subjected to fracture and TBI, we observed increased expression of *Vegfa* in the fracture callus also on day 3, but not on day 7 after surgery (Fig. 6D), correlating with elevated serum concentrations of VEGFA at the same time point (Fig. 6E). This was further supported by immunohistochemical

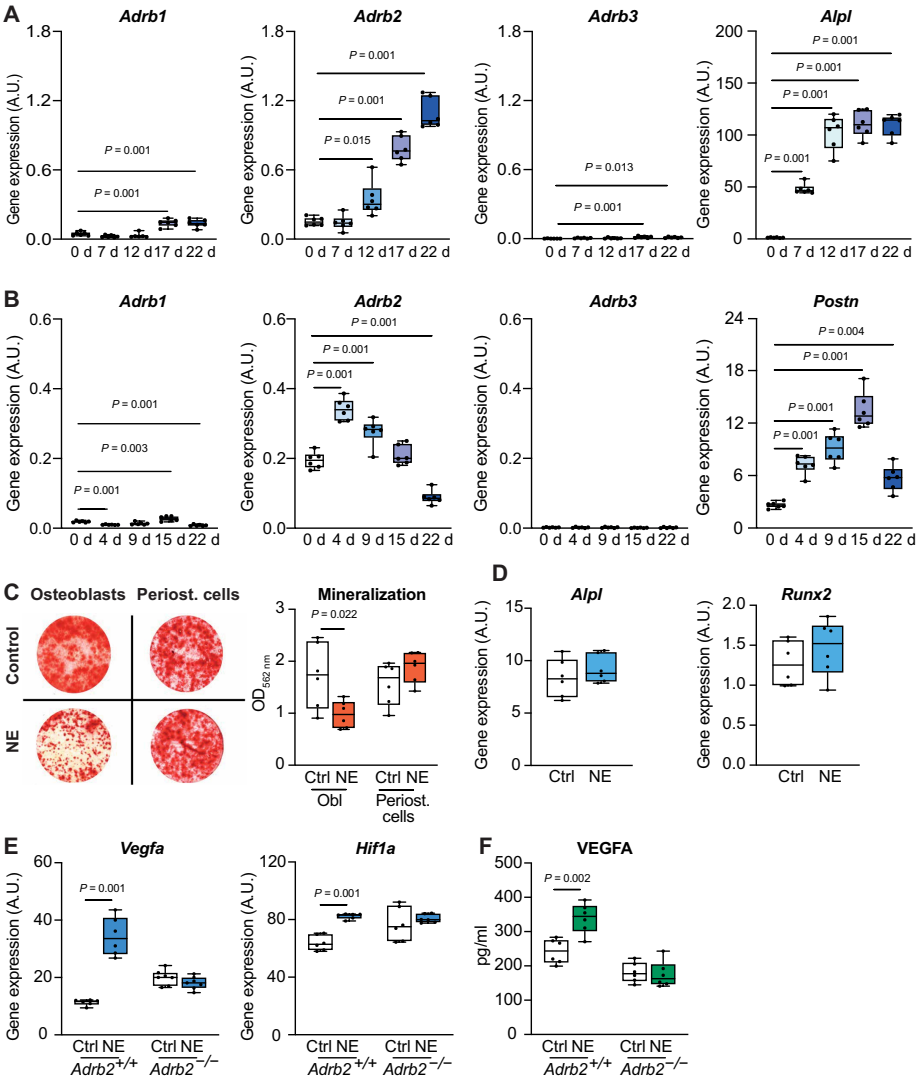

Fig. 5. NE-ADRB2 signaling induces VEGFA expression in periosteal cells. (**A**) Expression of *Adrb1*, *Adrb2*, *Adrb3*, and control osteoblast marker alkaline phosphatase (*Alpl*) in cultured murine bone marrow–derived osteoblasts during osteogenic differentiation in vitro as determined by qRT-PCR. (**B**) Expression of *Adrb1*, *Adrb2*, *Adrb3*, and control periosteal cell marker periostin (*Postn*) in murine primary periosteal cells at the indicated time points of differentiation in vitro. (**C**) Representative alizarin red–stained images of bone marrow–derived osteoblasts or primary periosteal cells and quantification of extracellular matrix mineralization after 15 days of osteogenic differentiation in vitro with or without NE. (**D** and **E**) Expression of the indicated genes in (D) WT or (E) WT and *Adrb2*$^{-/-}$ periosteal cells derived from femur at day 15 of differentiation stimulated with or without NE in vitro for 6 hours. (**F**) Enzyme-linked immunosorbent assay (ELISA) of VEGFA concentration in the supernatant of the same cultures. (A, B, D, and E) A.U., arbitrary copy number units per housekeeping gene. For (A) to (F), $n = 6$ independent cultures, and all cells were derived from murine femora. Data are presented as box plots with median and 25th and 75th quantiles, and whiskers indicate extremes. Data were analyzed by one-way ANOVA followed by Tukey's post hoc test (A and B) and two-tailed Student's *t* test (C to F).

staining with a VEGFA-specific antibody, demonstrating a higher signal intensity in the callus of TBI mice compared with sham controls (Fig. 6F and fig. S8B). VEGFA is pivotal to the formation of type-H vessels, which are characterized by the coexpression of CD31 and endomucin in regenerating bone (*33*, *34*). Therefore, we next studied type-H vessel formation at the end of the vascularization stage in fracture healing, corresponding to 14 days after osteotomy in mice. Here, *Adrb2*$^{-/-}$ mice showed more than a 50% reduction in the formation of type-H vessels in the callus at this time point (Fig. 6, G and H, and fig. S9A). In contrast, increased formation of type-H vessels was detected in the fracture callus of WT mice with a concomitant TBI at the same healing stage (Fig. 6, I and J, and fig. S9B).

NE-induced overexpression of VEGFA depends on the neuropeptide αCGRP

Previous studies demonstrated that VEGFA expression during bone regeneration is promoted by αCGRP, a vasoactive neuropeptide also essential for an adequate fracture healing process (*35*, *36*). In cultured periosteal cells, exposure to NE increased α*Cgrp* gene expression and CGRP protein content in culture supernatants (Fig. 7, A and B, and fig. S10, A and B). In vivo, α*Cgrp* mRNA expression in the fracture callus was increased after TBI in the early healing phase and associated with increased serum CGRP concentration 3 and 7 days after TBI in 12-week-old WT mice (Fig. 7, C and D). Similarly, serum CGRP concentration increased during fracture healing in WT mice; however, it remained unaltered in *Adrb2*$^{-/-}$ mice (Fig. 7E). These findings were confirmed locally in the fracture gap, where a reduced signal intensity of CGRP immunofluorescence was observed in *Adrb2*$^{-/-}$ mice 7 days after osteotomy, whereas the opposite was observed in mice with fracture and concomitant TBI (Fig. 7F). CGRP potentiated the stimulatory effect of NE on *Vegfa* expression in cultured WT periosteal cells (Fig. 7G). The CGRP receptor antagonist olcegepant (BIBN4096) inhibited the stimulatory effect of NE on *Vegfa* expression (Fig. 7H). Likewise, NE failed to induce *Vegfa* and *Hif1a* expression in periosteal cells lacking αCGRP (Fig. 7I and fig. S10C). Similar observations were made in bone marrow–derived

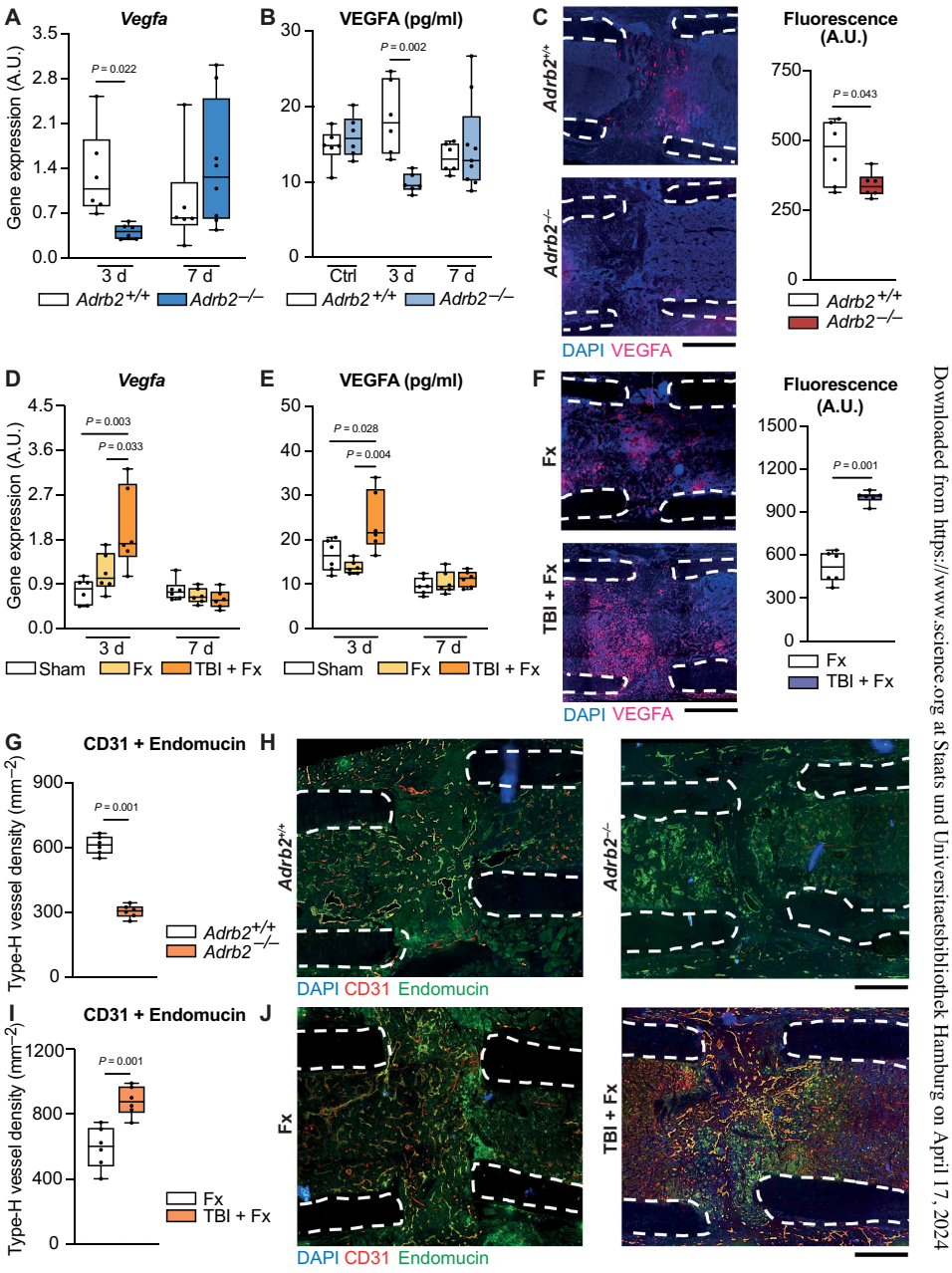

Fig. 6. NE-ADRB2 signaling controls VEGFA expression and type-H vessel formation in vivo. (**A**) Gene expression analysis by qRT-PCR of *Vegfa* in the callus 3 and 7 days after osteotomy in 30-week-old mice of the indicated genotypes. (**B**) Serum VEGFA concentrations in the same mice and untreated controls at the indicated time points. (**C**) Representative immunohistochemical staining for VEGFA (red) in the fracture callus of 30-week-old mice of the indicated genotypes 7 days after osteotomy, and quantification of signal intensity in the region of interest (ROI). Scale bar, 300 μm. (**D**) Gene expression analysis by qRT-PCR of *Vegfa* in the callus 3 and 7 days after osteotomy in 12-week-old WT mice with or without TBI in comparison with unfractured femoral midshafts in sham mice. (**E**) Serum VEGFA content in the same mice and sham-operated controls at the indicated time points. (**F**) Representative immunohistochemical staining for VEGFA in the fracture callus of 12-week-old WT mice 7 days after osteotomy with or without TBI and quantification of signal intensity in the ROI. Scale bar, 300 μm. (**G**) Quantification of type-H vessel density and (**H**) representative immunohistochemical staining for CD31 and endomucin in the fracture callus of 30-week-old mice of the indicated genotypes 14 days after osteotomy. Scale bar, 400 μm. (**I**) Quantification of type-H vessel density and (**J**) representative immunohistochemical costaining in the fracture callus of 12-week-old WT mice 14 days after osteotomy with or without TBI. Scale bar, 400 μm. In (C), (F), (H), and (J), dotted white lines show the fracture ends. (A and D) A.U., arbitrary copy number units per housekeeping gene. (C and F) A.U., arbitrary fluorescence units. For (A) and (C) to (J) $n = 6$ and for (B) $n = 6$ to 9 mice per group and time point as indicated by the individual data points. Numerical data are presented as box plots with median and 25th and 75th quantiles, and whiskers indicate extremes. Data were analyzed by Mann-Whitney *U* test (A), two-tailed Student's *t* test (B, C, F, G, and I), or one-way ANOVA followed by Tukey's post hoc test (D and E).

osteoblasts. NE-induced *Vegfa* and *Hif1a* expression was blunted in osteoblasts derived from $\alpha Cgrp^{-/-}$ mice (fig. S10D). Last, to test the functional relevance of these observations in vivo, $\alpha Cgrp^{-/-}$ mice were subjected to TBI. Like $Adrb2^{-/-}$ mice, $\alpha Cgrp^{-/-}$ animals did not have enhanced fracture healing with TBI as evidenced by radiological and histological outcomes (Fig. 7, J and K).

Pharmacological modulation of ADRB2 signaling controls type-H vessel formation and healing in regenerating bone

To test our findings for therapeutic relevance, we next used the nonselective ADRB2 antagonist propranolol (which blocks both β_1 and β_2 adrenoreceptors) (*37*), the selective β_1-adrenoreceptor antagonist atenolol (*38*), and the selective ADRB2 agonist formoterol (used as an inhaled agent in asthma or chronic obstructive pulmonary disease) (*39*). We first measured the effects of these drugs on the unfractured skeleton in naïve mice without osteotomy. Daily injections of propranolol for 3 weeks increased trabecular bone mass in spine and distal femur as evidenced by μCT scanning (fig. S11, A and B). Whereas the β_1-specific antagonist atenolol had no effect, formoterol treatment resulted in decreased trabecular numbers and increased trabecular separation; none of the treatments affected cortical thickness (fig. S11C). These findings were also confirmed by undecalcified

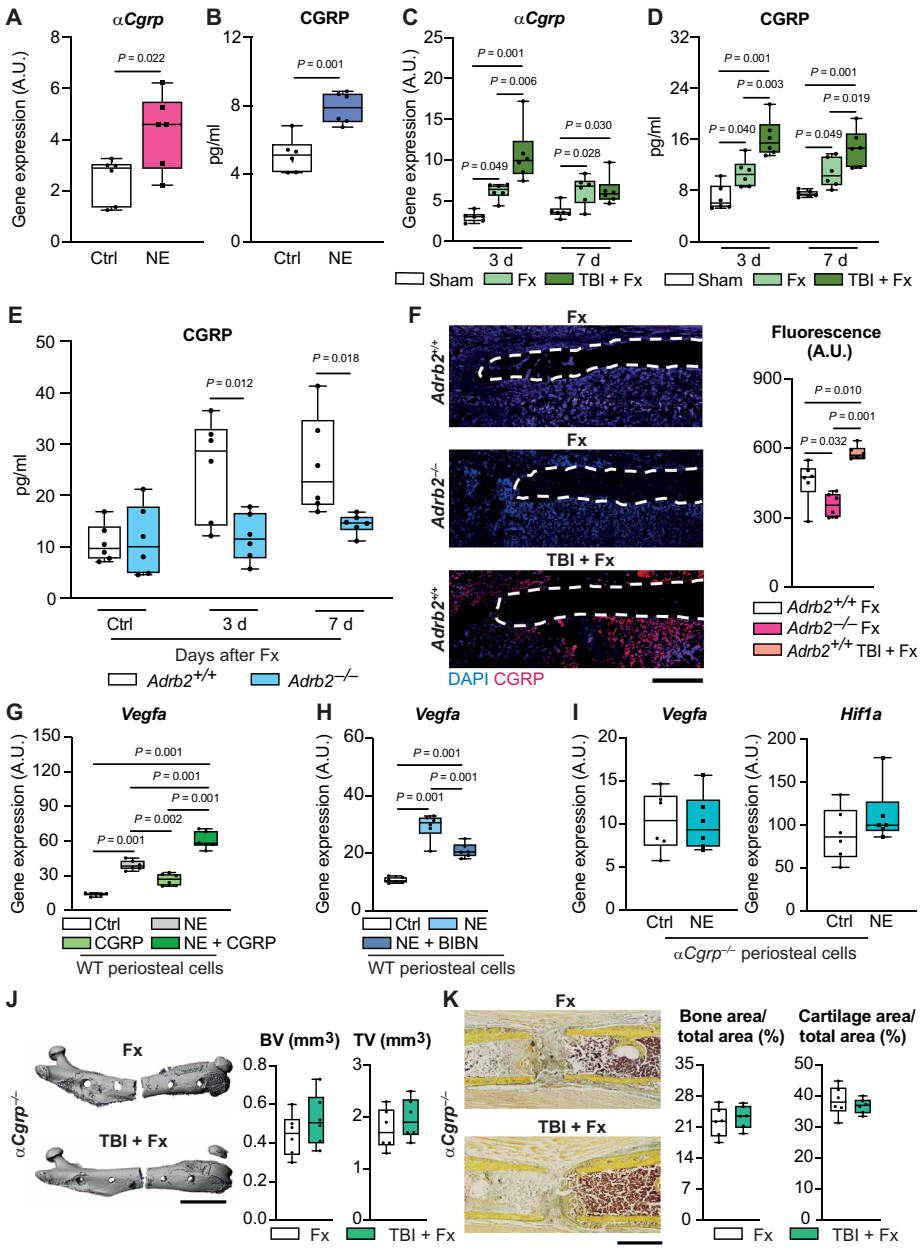

Fig. 7. Induction of *Vegfa* by NE depends on αCGRP. (**A**) Gene expression of α*Cgrp* by qRT-PCR in WT periosteal cells derived from femur after stimulation with NE for 6 hours and (**B**) CGRP protein concentrations in the supernatant of the same cultures measured by ELISA. (**C**) Gene expression of α*Cgrp* in the fracture callus of 12-week-old WT mice with fracture alone or TBI and fracture compared with unfractured femoral bone (Sham) and (**D**) CGRP concentrations in the serum of the same mice. (**E**) CGRP concentrations in the serum of 30-week-old mice of the indicated genotypes with or without fracture (Fx). (**F**) Representative immunohistochemical staining for CGRP in the fracture callus of 30-week-old mice of the indicated genotypes with a femoral osteotomy fracture model with or without TBI and quantification of signal intensity in the ROI 7 days after surgery. A.U., arbitrary fluorescence units. Dotted white lines show the fracture ends. Scale bar, 100 μm. (**G**) Gene expression analysis by qRT-PCR of *Vegfa* in WT periosteal cells stimulated with NE, CGRP, or both for 6 hours. (**H**) Gene expression of *Vegfa* in WT periosteal cells stimulated with NE with or without the CGRP receptor antagonist olcegepant (BIBN) for 6 hours. (**I**) Gene expression of *Vegfa* and *Hif1a* in α*Cgrp*$^{-/-}$ periosteal cells stimulated with NE for 6 hours. (**J**) Representative μCT images of the fractured femora in 12-week-old α*Cgrp*$^{-/-}$ mice with or without TBI 21 days after fracture and radiological quantification of callus BV and TV. Scale bar, 4 mm. (**K**) Representative callus sections stained with Movat Pentachrome and histomorphometric quantification of bone area per total area and cartilage area per total area of the fracture callus in the same mice. Scale bar, 500 μm. (A, C, and G to I) A.U., arbitrary copy number units per housekeeping gene. For (A), (B), and (G) to (I), $n = 6$ independent cultures per group. For (C) to (F), (J), and (K), $n = 6$ mice per group and time point. Data are presented as box plots with median and 25th and 75th quantiles, and whiskers indicate extremes. Data were analyzed by two-tailed Student's *t* test (A, B, E, J, and K), Mann-Whitney *U* test (I), or one-way ANOVA followed by Tukey's post hoc test (C, D, and F to H).

histology of lumbar spine, where bone volume was increased in the propranolol group and reduced in the formoterol group (fig. S12). Thereafter, we assessed the impact of propranolol, atenolol, and formoterol on fracture healing in adult mice. Using μCT scanning, we found that systemic propranolol treatment for 3 weeks impaired the formation of new bone in the callus, whereas systemic formoterol application resulted in improved radiological outcomes (Fig. 8A). In the case of atenolol treatment, no alterations in bone healing were observed. The same findings were made in undecalcified cryosections of the fracture callus, where propranolol treatment resulted in a reduction of newly formed bone, formoterol increased mineralized callus volume, and atenolol had no effect (Fig. 8B). Assessment of osseous callus bridging further demonstrated a high rate of fracture nonunion in mice treated with propranolol and improved fracture union in mice receiving formoterol (Fig. 8C). A decreased density of type-H vessels was detected in mice treated with propranolol, whereas the opposite effect was observed in the case of formoterol treatment (Fig. 8D and fig. S13). From a clinical perspective, we performed a retrospective cohort analysis of 72 polytraumatized patients with long bone shaft fractures (humerus, femur, or tibia), with 36 patients in the cohort receiving intravenous NE treatment for cardiovascular support. Patients with TBI or spinal cord injury were excluded because of a confounding effect on fracture healing. As controls, we assessed otherwise healthy patients with a corresponding long bone fracture only

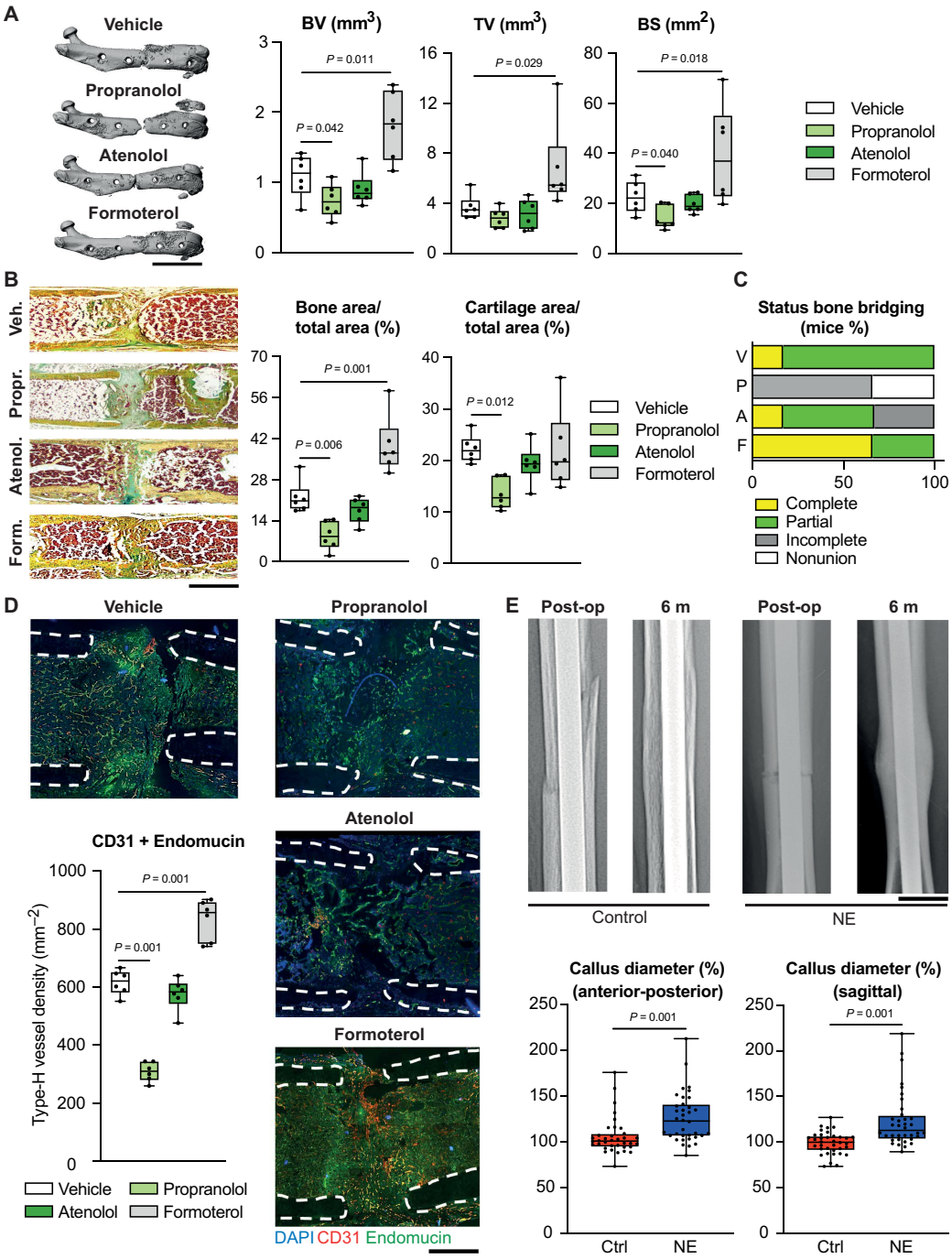

Fig. 8. ADRB2 agonism and antagonism modulate fracture healing. (**A**) Representative μCT images of the fractured femora in 30-week-old WT mice treated with daily intraperitoneal injections of vehicle, the β_1/β_2 antagonist propranolol, the β_1-specific antagonist atenolol, or the β_2-specific agonist formoterol during the entire study period (21 days) and quantification of callus BV, TV, and BS in the callus. Scale bar, 5 mm. (**B**) Representative callus sections in the same mice and quantification of bone area per total area and cartilage area per total area. Scale bar, 500 μm. (**C**) Semiquantitative evaluation of osseous callus bridging in the same mice. (**D**) Representative immunohistochemical staining for CD31 and endomucin in the fracture callus 14 days after osteotomy in the indicated treatment groups and quantification of type-H vessel density. Dotted white lines show the fracture ends; scale bar, 200 μm. (**E**) Representative radiographs of tibial fractures from patients with or without systemic NE treatment immediately postoperatively and 6 months (6 m) after intramedullary nailing and quantification of relative callus diameter in anterior-posterior and sagittal plane of the healed fractures (n = 36 patients per group). Scale bar, 15 mm. For (A) to (D), n = 6 mice per group and time point. (A), (B), (D), and (E) are presented as box plots with median and 25th and 75th quantiles, and whiskers indicate extremes. Data in (A), (B), and (D) were analyzed by one-way ANOVA followed by Tukey's post hoc test. Data in (E) were analyzed by Mann-Whitney U test because of nonparametric distribution.

(table S1). All patients received intramedullary nailing of the shaft fractures, and callus size was measured 6 months after surgery by two blinded investigators. Fracture patients who had received systemic NE treatment showed an increase in relative callus diameter in both the anterior-posterior and the sagittal planes (Fig. 8E).

DISCUSSION

In the search for approaches to pharmacologically improve bone healing and prevent fracture nonunion, we investigated the clinical phenomenon that TBI improves fracture healing but induces bone loss in the uninjured skeleton (*12*). Our data show that increased NE-ADRB2 signaling mediated TBI-induced bone remodeling and regeneration in mice. Furthermore, we demonstrate that ADRB2 plays an age-dependent and pharmacologically targetable role in fracture healing by promoting callus neovascularization under conditions of increased NE and enhanced sympathetic tone.

The clinical observation that TBI accelerates bone healing may hold the key to developing treatment approaches to improve fracture healing (*12*). This is particularly important because, unlike osteoporosis where antiresorptive and osteoanabolic agents are readily available, there are no pharmacologic options that reliably improve bone healing and prevent bone nonunion (*4, 6*). Intermittent injections of teriparatide, a fragment of human parathyroid hormone that promotes bone formation, have shown promising results in animal models, but compelling clinical studies supporting these observations are lacking (*40*). In addition, although topical application of bone morphogenetic proteins can potently stimulate osteogenesis and thus bone repair, their use is limited by serious adverse effects, including inflammatory tissue swelling with compression of nerve structures, ectopic bone formation, excessive osteolysis, and wound healing complications (*41*).

Callus is a very heterogeneous tissue consisting of a dynamically changing composition of many different cell types during overlapping healing stages; thus, attempts to decipher the molecular signature of bone regeneration after TBI have been largely inconclusive. We took advantage of the fact that TBI also affects bone remodeling in unfractured bone, which is much more homogeneous in tissue composition compared with callus. Unbiased RNA-seq not only showed reduced expression of osteoblast markers after TBI but also revealed suppressed expression of *Adrb2* in unfractured bone. ADRB2 is a G protein–coupled cell surface receptor that is down-regulated at the mRNA level upon stimulation with endogenous ligands (*22*), including NE, suggesting a hyperadrenergic state during TBI. In this regard, previous seminal work identified ADRB2, one of the major receptors for NE, as an essential regulator of both osteoclast and osteoblast function in mice (*7, 29, 42*). Stimulation of ADRB2 by NE inhibits osteoblast proliferation and bone formation (*43*). In addition, activation of ADRB2 in osteoblasts results in increased bone resorption through induction of RANKL, the master regulator of osteoclastogenesis (*44*). In our study, these previously described effects of NE-ADRB2 signaling were mirrored in the unfractured skeleton of mice with TBI. Mechanistically, the TBI-induced skeletal changes were abolished in $Adrb2^{-/-}$ mice, providing genetic evidence that, in the unfractured bone, TBI leads to the deterioration of bone remodeling through ADRB2.

In terms of fracture healing, the beneficial effect of TBI on bone regeneration was also absent in mice lacking ADRB2. This was unexpected because previous studies have reported inconsistent results regarding the role of β-adrenergic signaling in bone repair. Minkowitz *et al.* (*45*) reported that propranolol improved fracture union of bone defects filled with demineralized bone matrix powder in young rats. This was not confirmed in an independent study, in which propranolol failed to alter fracture healing in rats of an unreported age (*46*). Another study showed that local, but not systemic, inhibition of β-adrenergic signaling stimulated the healing of bone defects in rats of an unspecified age (*47*). Last, a more recent study suggested that a single preoperative injection of propranolol improved bone healing in a model of chronic psychosocial stress by modulating immune cell function in young mice (*48*).

Despite minor alterations in the early stages of bone healing observed only histologically but not radiographically, we reported normal bone regeneration in young $Adrb2^{-/-}$ mice 21 days after osteotomy. In contrast, adult $Adrb2^{-/-}$ mice exhibited impaired bone healing and a high rate of fracture nonunion. We detected increased NE content in the bones of adult mice, confirming previous studies demonstrating low local NE reuptake in cortical bone and consequently enhanced NE signaling (*31*). These findings are also consistent with an overall increased sympathetic tone in aged animals, which is well established not only in animal models but also in humans (*30*). Although of minor importance to bone repair in young and otherwise healthy mice, ADRB2 controls fracture healing under conditions of increased sympathetic tone, including TBI and aging.

Increased β-adrenergic signaling after TBI was also observed in another recent study, in which NE signaling was reported to shape the anti-inflammatory environment in the bone marrow through expansion of M2 macrophages (*49*). However, it remained unclear whether and how the described immunomodulatory effects of TBI translated into improved bone healing and affected the unfractured skeleton. Our data demonstrate that ADRB2 mediates TBI-induced bone loss in the unfractured mouse skeleton through the established role of ADRB2 as a direct inhibitor of osteoblastic bone formation and a promoter of osteoclastic bone resorption (*8*). Because this did not provide an explanation for the role of ADRB2 in promoting bone healing observed in both mice with TBI and otherwise healthy adult animals, we monitored the effects of NE on periosteal cells and showed high expression of ADRB2 in cortical bone in vivo. Whereas NE did not affect matrix mineralization in periosteal cells, it caused a direct ADRB2-dependent induction of the angiogenic factors *Vegfa* and *Hif1a*. Both mediators regulate the formation of type-H blood vessels, which are essential for new bone formation during fracture healing (*33*, *34*). Consequently, the callus of mice with TBI showed an increased density of type-H vessels, and adult $Adrb2^{-/-}$ mice exhibited the opposite vascular phenotype, suggesting that enhanced NE-ADRB2 signaling is a critical regulator of callus vascularization. That VEGFA was not reduced in unfractured bones from naïve adult $Adrb2^{-/-}$ mice further implies that physical disruption or an inflammatory response after bone injury is required for activation of ADRB2-dependent up-regulation of VEGFA in the skeleton.

The importance of callus vascularization in bone regeneration is best illustrated by several clinical studies demonstrating that vascular disease is a major risk factor for fracture nonunion (*33*, *50*). Similarly, damage to the periosteum, whose integrity is a prerequisite for sufficient callus vascularization, impairs bone healing (*51*). The neuropeptide αCGRP, which signals through the G protein–coupled calcitonin receptor–like receptor, is known to be highly expressed in the periosteum and essential for adequate fracture healing (*36*). Given that a previous study described a CGRP-dependent induction of

Vegfa expression during bone healing, we also tested the functional role of αCGRP in the stimulatory effect of NE on VEGFA expression (*35*). Like VEGFA, αCGRP was induced by NE in periosteal cells, and α*Cgrp*$^{-/-}$ mice showed no improved bone healing after TBI. Given that *Vegfa* induction by NE was blunted by the CGRP receptor antagonist olcegepant (BIBN4096), these observations suggest an autocrine mechanism by which CGRP modulates the stimulatory effect of NE on VEGFA expression. Although our study focused primarily on periosteal cells, we also found that NE-ADRB2 signaling increased *Vegfa* expression in osteoblasts. Thus, it is likely that increased NE signaling induces the production of angiogenic factors not only in periosteal cells but also in other cell types during bone repair, because ADRB2 has been repeatedly shown to be a positive regulator of angiogenesis in many organ systems (*52*). For example, NE dose- and time-dependently induces *Vegfa* transcription in brown adipocytes, which is reversible by the β-blocker propranolol (*53*, *54*). Similarly, adrenergic signaling through ADRB2 has been shown to promote VEGFA-dependent tumor vascularization in prostate, skin, and breast cancer cells (*55*–*57*). Together, these observations demonstrate that NE is capable of inducing VEGFA in a variety of different cell types and, in the case of bone healing, results in an overall promotion of type-H vessel formation required for osteogenesis.

From a translational perspective, we conducted a retrospective analysis of a cohort of patients with long bone fractures treated with intravenous NE. These patients received systemic NE for cardiovascular support after polytrauma with life-threatening injuries, which typically worsen fracture healing outcomes (*58*). The association of systemic NE treatment with increased bone callus formation 6 months after injury in this cohort provides suggestive evidence in support of our findings in mice, but there were a number of potential confounders in this clinical study, including comorbidities and injury scores. We treated adult WT mice with the selective ADRB2 agonist formoterol after inducing osteotomy. Systemic application of this drug, which is widely used clinically as an inhaled agent for asthma and chronic obstructive pulmonary disease, promoted type-H vessel formation and improved fracture healing, demonstrating that pharmacological ADRB2 agonism is a suitable approach to stimulate bone regeneration, at least in mice. Although these data identify the cell surface receptor ADRB2 as a promising target for promoting bone healing, they also suggest that its blockade may result in impaired fracture healing. Our observation that the nonselective β-blocker propranolol caused delayed fracture healing in adult mice is supported by the Steffenson *et al.* (*59*) study reporting a moderate association of β-blocker exposure with nonunion in 253,266 fracture cases. Given these findings and recent demographic trends, with >22% of people aged 60 years or older taking β-blockers (*60*), it is reasonable to examine the impact of this class of drugs on fracture nonunion in humans in more depth. Our data in fractured bone in mice and previous observations by the Karsenty group and others in unfractured bone suggest that ADRB2 mediates most of the effects of NE in mice (*29*, *44*). There is also clinical evidence supporting a predominant role for ADRB1 in the human skeleton (*61*). The ADRB1 antagonist atenolol did not affect fracture healing in our mouse study, suggesting potentially distinct roles for ADRB1 and ADRB2 in fracture healing.

Our study has several limitations, and further steps are needed to translate our findings into clinical practice. First, in accordance with the 3R principles (replace, reduce, refine), we used group sizes of $n = 6$ to 9 for the animal experiments. Therefore, subtle phenotypic changes, for example, in the bone and healing phenotypes of young *Adrb2*$^{-/-}$ mice, might not have been measurable because of the limited sample size. Second, we relied on a global ADRB2 deficiency mouse model. Although this does not affect the overall conclusions of this study, follow-up experiments in mice with conditional deletion of *Adrb2* in periosteal cells, osteoblasts, or other cell types are warranted to identify the precise cellular mechanism by which ADRB2 signaling affects neovascularization and fracture callus healing. Similarly, systemic application of formoterol is not an ideal approach to augment bone repair in humans because of potential cardiovascular adverse effects. Therefore, the development of technical means to locally activate ADRB2 in the event of a fracture, for example, by controlled drug release scaffolds or systemic ADRB2 agonists conjugated to specific targets expressed in regenerating bone, is required. Last, prospective clinical trials are warranted to examine whether β-blockers are suitable to prevent bone loss after TBI and whether their use is associated with impaired outcomes in bone healing. A National Institutes of Health (NIH)–funded randomized controlled trial is currently investigating the effect of β-blockers in the prevention of osteoporosis (*62*).

In summary, we have clarified the mechanism underlying the negative impact of TBI on intact bone, revealing that increased ADRB2 signaling after TBI has an inhibitory effect on bone formation. Moreover, our results unexpectedly identified an important function of ADRB2 signaling in the injured mouse skeleton. We show that under conditions of enhanced sympathetic tone due to increased NE release, such as in TBI or, most commonly, as a physiological adaptation in the aging organism (*30*), ADRB2 signaling is an essential stimulus for bone healing. It is currently still unclear whether nonunion differs with age in humans (*63*), and some studies have even reported lower rates of fracture nonunion in healthy elderly patients compared with young patients with lower sympathetic tone (*64*–*66*). Further studies are warranted to examine the potential clinical implications of our findings regarding improved fracture healing in mice with TBI.

MATERIALS AND METHODS

Study design

The aim of this study was to investigate the effects of TBI on fracture healing and bone metabolism in mice. To dissect functional pathways including the roles of ADRB2 and αCGRP, we used mice that were subjected to genetic or pharmacological modification. Genetically modified models included mice with a global deletion of *Adrb2* or α*Cgrp*, respectively. For pharmacologic proof-of-principle experiments, WT mice were systemically treated with the ADRB1/2 antagonist propranolol, the ADRB1-specific antagonist atenolol, or the ADRB2-specific agonist formoterol. Bone volume per tissue volume (for uninjured bone) and bone volume (for injured bone) was measured by μCT and was used as the primary end point; secondary end points were prospectively developed during the study. For in vivo experiments, sample sizes were calculated on the basis of our previous work according to the method in www.lasec.cuhk.edu.hk/sample-size-calculation.html, with a statistical power of 80% and a level of significance of 0.05. This resulted in group sizes of at least $n = 6$ mice per group for each time point. For all animal experiments, directly compared groups such as sham, isolated fracture, or fracture in combination with TBI were performed in parallel and treated equally throughout the experiment. Littermates were randomized to the different experimental groups, and all biological samples were coded to facilitate blinded evaluation. Health status was controlled daily, using

predefined score sheets and humane end points, whereby no animal had to be excluded. Underlying molecular pathways were further examined by the cultivation and stimulation of different murine primary cells. For the corresponding in vitro studies, the a priori sample size calculation was performed as for the in vivo experiments, with fold change gene expression as the primary end point. Using the results of our previous work, this yielded a group size of $n = 6$ biologically independent cultures. For the in vitro sample evaluation process, investigators were blinded during sample processing and analysis of outcome measures. The association of systemic NE treatment with bone regeneration in patients with long bone fractures was determined by measuring the callus diameter on digitally recorded radiographs.

All experimental procedures were approved by the local legal representative animal rights protection authorities (Landesamt für Gesundheit und Soziales Berlin, G0009/12; G0007/2017; G0147/2018; G0112/2022 and Behörde für Justiz und Verbraucherschutz Hamburg, N085/2020; N062/2023; N118/2023) and were performed according to the principles established by the NIH *Guide for the Care and Use of Laboratory Animals* as well as the Welfare Act (Federal Law Gazette I, p.1094). The anonymized retrospective clinical study was approved by the local ethics committee of the Charité—Universitätsmedizin Berlin, Campus Virchow Klinikum (EA4/038/17).

Retrospective clinical observational study

Medical records of all patients admitted to Charité—Universitätsmedizin Berlin, Campus Virchow Klinikum, and diagnosed with a traumatic shaft fracture of the humerus, femur, or tibia [A1 to A3 and B1 to B3 according to (*67*)] between 2008 and 2022 were identified by patient management software (SAP Business Client 6.5, SAP Walldorf). Inclusion criteria were traumatic midshaft fractures of the humerus, femur, or tibia that were surgically stabilized with an intramedullary nail and recorded radiographic follow-up for 6 months. Exclusion criteria were pathologic fractures; no 6-month radiographic follow-up; and no recorded Injury Severity Score (ISS), TBI, or spinal cord injury. A total of 850 patients were identified. Fifty-seven patients were excluded because of concomitant TBI or spinal cord injury. Six hundred five patients were excluded because they were lost to follow-up or had pathologic fractures. One hundred eighty-eight patients were finally identified, of whom 36 had received NE therapy during their intensive care unit (ICU) stay and 152 had not. Propensity score matching for age, sex, and American Society of Anesthesiologists (ASA) score was performed in R software using the MatchIt package (RStudio) to create balanced and homogeneous groups. This resulted in a total of 72 patients, 36 patients with and 36 patients without systemic NE therapy ($n = 3$ humerus fractures, $n = 16$ femoral fractures, $n = 17$ tibial fractures per group). Fracture healing was analyzed radiologically by measuring the maximum diameter of callus formation on anterior-posterior and sagittal radiographs 6 months postoperatively using radiographic calibration markers. The measurements were then divided by the maximum diameter of the fracture site measured on radiographs 1 week after surgery to calculate the resulting relative increase in callus growth.

Animals

WT mice with FVB/129 or C57Bl/6J background were used at the age of 12 (young) or 30 (adult) weeks as indicated. *Adrb2*$^{-/-}$ mice (*Adrb2tm1Bkk/J*; the Jackson Laboratory, no. 031496) exhibited FVB/129 genetic background, and α*Cgrp*$^{-/-}$ mice (*Calcatm1Eme*; MGI, no. 21485389) exhibited C57Bl/6J genetic background (both lines backcrossed at least seven times) (*68*). The animals were maintained under standard conditions (12-hour light-dark circadian rhythm, 22°C) in a specific pathogen–free facility and housed in stable groups. Water and a standard diet were provided ad libitum. In line with the animal welfare act, to reduce the total number of bred mice, male mice were used for the investigation of isolated fracture healing in *Adrb2*$^{-/-}$ mice and for the treatment experiments with propranolol, atenolol, and formoterol. For all experiments involving TBI, female mice were used. To control for potential sex differences, the impact of ADRB2 deficiency on isolated fracture healing was confirmed in female mice, whereas the ADRB2-dependent effect of TBI on fracture healing was confirmed in male mice with similar results. Directly compared groups always had the same sex.

Surgery

Mice received a femoral osteotomy stabilized with an external fixator as previously described (*69*). Briefly, the mice were anesthetized with isoflurane, and the right femur was exposed. An external fixator (RI-System) was mounted on the femur, using four pins and a 0.45-mm hand drill. The fracture gap was created using a 0.7-mm-diameter Gigli wire saw. The wound was closed with a simple interrupted suture. TBI to the left parietotemporal cortex was induced as previously described (*20*). After the craniotomy, a controlled cortical impact (bolt 3 mm flat, 45° angle, impact velocity of 3.5 m s^{-1}, 0.25 mm penetration depth, contact duration of 0.15 s) was induced on the intact dura mater. Subsequently, the skull piece was repositioned and fixed with dental cementum, and the skin incision was closed with Ethilon 6.0 suture. For sham surgery, the same protocol was followed, except for the controlled cortical impact onto the dura mater. For the combination of both injuries, TBI was induced before the fracture. Clindamycin (150 mg kg^{-1}, Hikma Pharma GmbH) and buprenorphine (0.1 mg kg^{-1}, Richter Pharma AG) were administered preoperatively. For optimal pain relief, metamizole (1 mg ml^{-1}, Novaminsulfon-ratiopharm) or Tramal (0.3 mg ml^{-1}, Grünenthal) was administered in the drinking water for 3 days postoperatively.

Pharmacological treatment

From the time point of surgery until euthanasia, the mice with fractures received two intraperitoneal injections daily of either vehicle (0.9% saline), propranolol hydrochloride (20 mg kg^{-1} for the first 5 days and 10 mg kg^{-1} from day 6 until euthanasia, Merck), atenolol (10 mg kg^{-1}, Merck), or formoterol fumarate dihydrate (10 mg kg^{-1}, Merck), diluted in 0.9% saline, with a total volume of 100 μl intraperitoneally. The mice were euthanized on postoperative day 14 or 21 as indicated. For naïve animals (no osteotomy), the mice received the same treatment daily for 21 days before euthanasia.

Microcomputed tomography

Fractured femora were fixed in 4% paraformaldehyde at 4°C for 24 hours. After removing the fixators, the bones were washed three times and stored in phosphate-buffered saline (PBS) during μCT scanning. Both fractured and unfractured femora were scanned using μCT (VivaCT 80, SCANCO Medical AG, Brüttisellen, Switzerland) with a voxel resolution of 15.6 μm, 400-ms integration time, 70 kVp, and 113 μA. The callus evaluation was performed in a volume of interest of 1 mm by 2 mm by 2 mm around the fracture gap. Data are presented according to the American Society for Bone and Mineral Research (ASBMR) guidelines for μCT analysis (*70*). For evaluation

of unfractured femora, a 1- to 2-mm midshaft and 1- to 2-mm distal segment were analyzed. Cortical and trabecular properties were derived using an automated image analysis algorithm provided by the manufacturer.

Biomechanics

After μCT evaluation, all bones harvested on day 28 were challenged with a destructive three-point bending test as previously described (*71*). In brief, femora were placed on two support bars of the device (ZwickRoell), and a bending load with a maximum of 20 N was applied medially onto the callus site. Derived parameters were calculated automatically by the device software.

Cryo-embedding

After μCT scans, the bones were incubated in ascending sucrose gradient (10, 20, and 30% each for 24 hours at 4°C) and embedded in super cryo-embedding medium (Section-Lab Co. Ltd.), frozen in hexane (Carl Roth GmbH & Co. KG), and stored at −80°C until further processing. Using a cryostat (Leica CM3050S, Leica Microsystems), longitudinal sections of 5 to 7 μm were prepared and mounted onto microscope slides using cryofilm (Cryofilm type II C, Section-Lab Co. Ltd.).

Cell culture

Female and male WT and mutant mice at the age of 12 to 18 weeks were used. For the generation of bone marrow–derived osteoblasts, long bones (femora) were cut open above the distal metaphysis, and the bone marrow was extracted by centrifugation (6000 rpm for 30 s). To remove tissue debris, the bone marrow was then filtered through a 70-μm cell strainer. For periosteal cell culture, epiphyses of the femora were removed, and bones were flushed out several times to remove the bone marrow. In the case of calvariae, the bones were dissected free of connective tissue. Digestion of periosteal tissue from femora and calvariae was then performed by incubation with 0.1% dispase (Roche Diagnostics GmbH) and 0.25% collagenase II (Gibco Life Technologies Corporation) at 37°C for 3 hours. Periosteal cells were separated using a 70-μm cell strainer and centrifuged at 1000 rpm for 10 min. Subsequently, the cells were plated onto 12-well plates in a concentration of 1×10^4 cells per well. α-Minimum essential medium (Merck KgaA) supplemented with 10% fetal calf serum was used for cultivation and changed every 2 to 3 days. Osteoblast differentiation was induced through stimulation with ascorbic acid (25 μg ml^{-1}) and 5 mM β-glycerophosphate when cells had reached 70% confluence for 10 days. For alizarin red staining, the cells were incubated with 40 mM alizarin red staining solution (pH 4.2) for 10 min at room temperature after fixation in 90% ethanol. To quantify alizarin red incorporation, the cells were washed with PBS and fixed in 90% ethanol for 1 hour. After additional washing, the cell-bound alizarin red was dissolved in 10% acetic acid. After incubation for 30 min at room temperature and 10 min at 85°C, the supernatant of a subsequent centrifugation step was neutralized with 10% ammonium hydroxide solution, and the absorbance was measured at 405 nm. For short- and long-term stimulations of periosteal cells and osteoblasts, the following conditions were used: NE (Arterenol, Cheplapharm, no. 03870227, 10^{-5} M), BIBN4096 (Tocris, no. 4561, 10^{-3} M), and recombinant mouse CGRP (Bachem, no. H-2265, 10^{-7} M).

Statistical analysis

All data were tested for normality by the Kolmogorov-Smirnoff test. Unpaired two-tailed Student's *t* test (parametric data) or Mann-Whitney *U* test (nonparametric data) was used for simple comparisons. For comparisons of more than two groups, data were analyzed by one-way analysis of variance (ANOVA) test, followed by Tukey's post hoc tests. Clinical data were assessed by Mann-Whitney *U* test. Numerical data are graphed in boxplots with median and 25th and 75th quantiles; whiskers indicate upper and lower extremes, respectively. The significance level was set at $P < 0.05$, with all *P* values reported in the figures (GraphPad Prism 9.1.1). All individual-level data are available in data file S1.

Supplementary Materials

This PDF file includes:
Materials and Methods
Figs. S1 to S13
Table S1
References (*72*–*77*)

Other Supplementary Material for this manuscript includes the following:
Data file S1
MDAR Reproducibility Checklist

REFERENCES AND NOTES

1. J. E. Compston, M. R. McClung, W. D. Leslie, Osteoporosis. *Lancet* **393**, 364–376 (2019).
2. G. F. Collaborators, Global, regional, and national burden of bone fractures in 204 countries and territories, 1990–2019: A systematic analysis from the Global Burden of Disease Study 2019. *Lancet Healthy Longev.* **2**, e580–e592 (2021).
3. B. Wildemann, A. Ignatius, F. Leung, L. A. Taitsman, R. M. Smith, R. Pesántez, M. J. Stoddart, R. G. Richards, J. B. Jupiter, Non-union bone fractures. *Nat. Rev. Dis. Primers* **7**, 57 (2021).
4. G. Russow, D. Jahn, J. Appelt, S. Märdian, S. Tsitsilonis, J. Keller, Anabolic therapies in osteoporosis and bone regeneration. *Int. J. Mol. Sci.* **20**, 83 (2019).
5. G. Marongiu, A. Dolci, M. Verona, A. Capone, The biology and treatment of acute long-bones diaphyseal fractures: Overview of the current options for bone healing enhancement. *Bone Rep.* **12**, 100249 (2020).
6. C. W. Schlickewei, H. Kleinertz, D. M. Thiesen, K. Mader, M. Priemel, K.-H. Frosch, J. Keller, Current and future concepts for the treatment of impaired fracture healing. *Int. J. Mol. Sci.* **20**, 5805 (2019).
7. S. Takeda, F. Elefteriou, R. Levasseur, X. Liu, L. Zhao, K. L. Parker, D. Armstrong, P. Ducy, G. Karsenty, Leptin regulates bone formation via the sympathetic nervous system. *Cell* **111**, 305–317 (2002).
8. G. Karsenty, S. Khosla, The crosstalk between bone remodeling and energy metabolism: A translational perspective. *Cell Metab.* **34**, 805–817 (2022).
9. C. Kesavan, N. M. Bajwa, H. Watt, S. Mohan, Experimental repetitive mild traumatic brain injury induces deficits in trabecular bone microarchitecture and strength in mice. *Bone Res.* **5**, 17042 (2017).
10. R. D. Brady, S. R. Shultz, M. Sun, T. Romano, C. van der Poel, D. K. Wright, J. D. Wark, T. J. O'Brien, B. L. Grills, S. J. McDonald, Experimental traumatic brain injury induces bone loss in rats. *J. Neurotrauma* **33**, 2154–2160 (2016).
11. N. M. Bajwa, C. Kesavan, S. Mohan, Long-term consequences of traumatic brain injury in bone metabolism. *Front. Neurol.* **9**, 115 (2018).
12. M. Hofman, G. Koopmans, P. Kobbe, M. Poeze, H. Andruszkow, P. R. G. Brink, H.-C. Pape, Improved fracture healing in patients with concomitant traumatic brain injury: Proven or not? *Mediators Inflamm.* **2015**, 204842 (2015).
13. H. E. Hinson, K. N. Sheth, Manifestations of the hyperadrenergic state after acute brain injury. *Curr. Opin. Crit. Care* **18**, 139–145 (2012).
14. J. Qian, X. Min, F. Wang, Y. Xu, W. Fang, Paroxysmal sympathetic hyperactivity in adult patients with brain injury: A systematic review and meta-analysis. *World Neurosurg.* **166**, 212–219 (2022).
15. A. P. Di Battista, S. G. Rhind, M. G. Hutchison, S. Hassan, M. Y. Shiu, K. Inaba, J. Topolovec-Vranic, A. C. Neto, S. B. Rizoli, A. J. Baker, Inflammatory cytokine and chemokine profiles are associated with patient outcome and the hyperadrenergic state following acute brain injury. *J. Neuroinflammation* **13**, 40 (2016).
16. S. B. Rizoli, B. N. R. Jaja, A. P. Di Battista, S. G. Rhind, A. C. Neto, L. da Costa, K. Inaba, L. T. da Luz, B. Nascimento, A. Perez, A. J. Baker, A. L. de Oliveira Manoel, Catecholamines as outcome markers in isolated traumatic brain injury: The COMA-TBI study. *Crit. Care* **21**, 37 (2017).
17. F. Driessler, P. A. Baldock, Hypothalamic regulation of bone. *J. Mol. Endocrinol.* **45**, 175–181 (2010).

18. Y. Song, L. Bi, Z. Zhang, Z. Huang, W. Hou, X. Lu, P. Sun, Y. Han, Increased levels of calcitonin gene-related peptide in serum accelerate fracture healing following traumatic brain injury. *Mol. Med. Rep.* **5**, 432–438 (2012).
19. Y. Song, G. X. Han, L. Chen, Y. Z. Zhai, J. Dong, W. Chen, T. S. Li, H. Y. Zhu, The role of the hippocampus and the function of calcitonin gene-related peptide in the mechanism of traumatic brain injury accelerating fracture-healing. *Eur. Rev. Med. Pharmacol. Sci.* **21**, 1522–1531 (2017).
20. S. Tsitsilonis, R. Seemann, M. Misch, F. Wichlas, N. P. Haas, K. Schmidt-Bleek, C. Kleber, K.-D. Schaser, The effect of traumatic brain injury on bone healing: An experimental study in a novel in vivo animal model. *Injury* **46**, 661–665 (2015).
21. E. Hinoi, N. Gao, D. Y. Jung, V. Yadav, T. Yoshizawa, M. G. Myers, S. C. Chua, J. K. Kim, K. H. Kaestner, G. Karsenty, The sympathetic tone mediates leptin's inhibition of insulin secretion by modulating osteocalcin bioactivity. *J. Cell Biol.* **183**, 1235–1242 (2008).
22. A. Mahmood, K. Ahmed, Y. Zhang, β-Adrenergic receptor desensitization/down-regulation in heart failure: A friend or foe? *Front. Cardiovasc. Med.* **9**, 925692 (2022).
23. H. Hörtnagl, A. F. Hammerle, J. M. Hackl, T. Brücke, E. Rumpl, H. Hörtnagl, The activity of the sympathetic nervous system following severe head injury. *Intensive Care Med.* **6**, 169–177 (1980).
24. G. L. Clifton, C. S. Robertson, K. Kyper, A. A. Taylor, R. D. Dhekne, R. G. Grossman, Cardiovascular response to severe head injury. *J. Neurosurg.* **59**, 447–454 (1983).
25. R. W. Hamill, P. D. Woolf, J. V. McDonald, L. A. Lee, M. Kelly, Catecholamines predict outcome in traumatic brain injury. *Ann. Neurol.* **21**, 438–443 (1987).
26. G. L. Clifton, M. G. Ziegler, R. G. Grossman, Circulating catecholamines and sympathetic activity after head injury. *Neurosurgery* **8**, 10–14 (1981).
27. P. D. Woolf, R. W. Hamill, L. A. Lee, J. V. McDonald, Free and total catecholamines in critical illness. *Am. J. Physiol.* **254**, E287–E291 (1988).
28. J. P. Desborough, The stress response to trauma and surgery. *Br. J. Anaesth.* **85**, 109–117 (2000).
29. D. Kajimura, E. Hinoi, M. Ferron, A. Kode, K. J. Riley, B. Zhou, X. E. Guo, G. Karsenty, Genetic determination of the cellular basis of the sympathetic regulation of bone mass accrual. *J. Exp. Med.* **208**, 841–851 (2011).
30. P. Balasubramanian, D. Hall, M. Subramanian, Sympathetic nervous system as a target for aging and obesity-related cardiovascular diseases. *Geroscience* **41**, 13–24 (2019).
31. Y. Zhu, Y. Ma, F. Elefteriou, Cortical bone is an extraneuronal site of norepinephrine uptake in adult mice. *Bone Rep.* **9**, 188–198 (2018).
32. T. Wang, X. Zhang, D. D. Bikle, Osteogenic differentiation of periosteal cells during fracture healing. *J. Cell. Physiol.* **232**, 913–921 (2017).
33. S. Stegen, N. van Gastel, G. Carmeliet, Bringing new life to damaged bone: The importance of angiogenesis in bone repair and regeneration. *Bone* **70**, 19–27 (2015).
34. A. P. Kusumbe, S. K. Ramasamy, R. H. Adams, Coupling of angiogenesis and osteogenesis by a specific vessel subtype in bone. *Nature* **507**, 323–328 (2014).
35. L. Ye, J. Xu, J. Mi, X. He, Q. Pan, L. Zheng, H. Zu, Z. Chen, B. Dai, X. Li, Q. Pang, L. Zou, L. Zhou, L. Huang, W. Tong, G. Li, L. Qin, Biodegradable magnesium combined with distraction osteogenesis synergistically stimulates bone tissue regeneration via CGRP-FAK-VEGF signaling axis. *Biomaterials* **275**, 120984 (2021).
36. J. Appelt, A. Baranowsky, D. Jahn, T. Yorgan, P. Köhli, E. Otto, S. K. Farahani, F. Graef, M. Fuchs, A. Herrera, M. Amling, T. Schinke, K.-H. Frosch, G. N. Duda, S. Tsitsilonis, J. Keller, The neuropeptide calcitonin gene-related peptide alpha is essential for bone healing. *EBioMedicine* **59**, 102970 (2020).
37. Ł. Wołowiec, G. Grześk, J. Osiak, A. Wijata, M. Mędlewska, P. Gaborek, J. Banach, A. Wołowiec, M. Głowacka, Beta-blockers in cardiac arrhythmias—Clinical pharmacologist's point of view. *Front. Pharmacol.* **13**, 1043714 (2022).
38. D. Ladage, R. H. G. Schwinger, K. Brixius, Cardio-selective beta-blocker: Pharmacological evidence and their influence on exercise capacity. *Cardiovasc. Ther.* **31**, 76–83 (2013).
39. M. Mintz, I. Barjaktarevic, D. A. Mahler, B. Make, N. Skolnik, B. Yawn, B. Zeyzus-Johns, N. A. Hanania, Reducing the risk of mortality in chronic obstructive pulmonary disease with pharmacotherapy: A narrative review. *Mayo Clin. Proc.* **98**, 301–315 (2023).
40. S. Babu, N. A. Sandiford, M. Vrahas, Use of teriparatide to improve fracture healing: What is the evidence? *World J. Orthop.* **6**, 457–461 (2015).
41. A. W. James, G. LaChaud, J. Shen, G. Asatrian, V. Nguyen, X. Zhang, K. Ting, C. Soo, A review of the clinical side effects of bone morphogenetic protein-2. *Tissue Eng. Part B Rev.* **22**, 284–297 (2016).
42. P. Ducy, M. Amling, S. Takeda, M. Priemel, A. F. Schilling, F. T. Beil, J. Shen, C. Vinson, J. M. Rueger, G. Karsenty, Leptin inhibits bone formation through a hypothalamic relay: A central control of bone mass. *Cell* **100**, 197–207 (2000).
43. L. Fu, M. S. Patel, A. Bradley, E. F. Wagner, G. Karsenty, The molecular clock mediates leptin-regulated bone formation. *Cell* **122**, 803–815 (2005).
44. F. Elefteriou, J. D. Ahn, S. Takeda, M. Starbuck, X. Yang, X. Liu, H. Kondo, W. G. Richards, T. W. Bannon, M. Noda, K. Clement, C. Vaisse, G. Karsenty, Leptin regulation of bone resorption by the sympathetic nervous system and CART. *Nature* **434**, 514–520 (2005).
45. B. Minkowitz, A. L. Boskey, J. M. Lane, H. S. Pearlman, V. J. Vigorita, Effects of propranolol on bone metabolism in the rat. *J. Orthop. Res.* **9**, 869–875 (1991).
46. P. Smitham, L. Crossfield, G. Hughes, A. Goodship, G. Blunn, C. Chenu, Low dose of propranolol does not affect rat osteotomy healing and callus strength. *J. Orthop. Res.* **32**, 887–893 (2014).
47. H. Wu, Y. Song, J. Li, X. Lei, S. Zhang, Y. Gao, P. Cheng, B. Liu, S. Miao, L. Bi, L. Yang, G. Pei, Blockade of adrenergic β-receptor activation through local delivery of propranolol from a 3D collagen/polyvinyl alcohol/hydroxyapatite scaffold promotes bone repair in vivo. *Cell Prolif.* **53**, e12725 (2020).
48. M. Haffner-Luntzer, S. Foertsch, V. Fischer, K. Prystaz, M. Tschaffon, Y. Mödinger, C. S. Bahney, R. S. Marcucio, T. Miclau, A. Ignatius, S. O. Reber, Chronic psychosocial stress compromises the immune response and endochondral ossification during bone fracture healing via β-AR signaling. *Proc. Natl. Acad. Sci. U.S.A.* **116**, 8615–8622 (2019).
49. W. Liu, W. Chen, M. Xie, C. Chen, Z. Shao, Y. Zhang, H. Zhao, Q. Song, H. Hu, X. Xing, X. Cai, X. Deng, X. Li, P. Wang, G. Liu, L. Xiong, X. Lv, Y. Zhang, Traumatic brain injury stimulates sympathetic tone-mediated bone marrow myelopoiesis to favor fracture healing. *Signal Transduct. Target. Ther.* **8**, 260 (2023).
50. H. Schmal, M. Brix, M. Bue, A. Ekman, N. Ferreira, H. Gottlieb, S. Kold, A. Taylor, P. Toft Tengberg, I. Ban, Nonunion—Consensus from the 4th annual meeting of the Danish Orthopaedic Trauma Society. *EFORT Open Rev.* **5**, 46–57 (2020).
51. B. P. Patro, M. Rath, D. Mohapatra, S. Kumar Patra, M. Chandra Sahu, G. Das, J. Sahoo, Traumatized periosteum: Its histology, viability, and clinical significance. *Orthop. Rev.* **14**, 30044 (2022).
52. A. Xanthopoulos, I. Daskalopoulou, S. Frountzi, E. Papadimitriou, A systematic review on the role of adrenergic receptors in angiogenesis regulation in health and disease. *Int. J. Transl. Med.* **1**, 353–365 (2021).
53. J. M. Fredriksson, J. M. Lindquist, G. E. Bronnikov, J. Nedergaard, Norepinephrine induces vascular endothelial growth factor gene expression in brown adipocytes through a beta -adrenoreceptor/cAMP/protein kinase A pathway involving Src but independently of Erk1/2. *J. Biol. Chem.* **275**, 13802–13811 (2000).
54. H. Yamashita, N. Sato, T. Kizaki, S. Oh-ishi, M. Segawa, D. Saitoh, Y. Ohira, H. Ohno, Norepinephrine stimulates the expression of fibroblast growth factor 2 in rat brown adipocyte primary culture. *Cell Growth Differ.* **6**, 1457–1462 (1995).
55. H. Chen, D. Liu, Z. Yang, L. Sun, Q. Deng, S. Yang, L. Qian, L. Guo, M. Yu, M. Hu, M. Shi, N. Guo, Adrenergic signaling promotes angiogenesis through endothelial cell-tumor cell crosstalk. *Endocr. Relat. Cancer* **21**, 783–795 (2014).
56. K. Lu, M. Bhat, S. Peters, R. Mitra, T. Oberyszyn, S. Basu, Suppression of beta 2 adrenergic receptor actions prevent UVB mediated cutaneous squamous cell tumorigenesis through inhibition of VEGF-A induced angiogenesis. *Mol. Carcinog.* **60**, 172–178 (2021).
57. Adrenergic nerves may promote angiogenesis in prostate cancer. *Cancer Discov.* **7**, 1366 (2017).
58. H. C. Pape, S. Halvachizadeh, L. Leenen, G. D. Velmahos, R. Buckley, P. V. Giannoudis, Timing of major fracture care in polytrauma patients - An update on principles, parameters and strategies for 2020. *Injury* **50**, 1656–1670 (2019).
59. L. Steffenson, B. Martin, A. Kantor, D. O'Neill, L. Myhre, T. Thorne, D. Rothberg, T. Higgins, J. Haller, L. Marchand, Beta-blocker exposure is associated with nonunion in a geriatric cohort of 253,266 extremity fractures. medRxiv 23292608 [Preprint] (2023). https://doi.org/10.1101/2023.07.14.23292608.
60. C. M. Hales, J. Servais, C. B. Martin, D. Kohen, Prescription drug use among adults aged 40-79 in the United States and Canada. *NCHS Data Brief*, no. 347 (National Center for Health Statistics, 2019); www.cdc.gov/nchs/products/databriefs/db347.htm.
61. S. Khosla, M. T. Drake, T. L. Volkman, B. S. Thicke, S. J. Achenbach, E. J. Atkinson, M. J. Joyner, C. J. Rosen, D. G. Monroe, J. N. Farr, Sympathetic β1-adrenergic signaling contributes to regulation of human bone metabolism. *J. Clin. Invest.* **128**, 4832–4842 (2018).
62. S. Khosla, D. M. Black, C. J. Rosen, E. J. Shane, Beta1-selective blockade for prevention of postmenopausal bone loss: A randomized controlled trial. NIH Report 1R01AG065154-01A1 (2021).
63. D. Saul, S. Khosla, Fracture healing in the setting of endocrine diseases, aging, and cellular senescence. *Endocr. Rev.* **43**, 984–1002 (2022).
64. R. Zura, M. J. Braid-Forbes, K. Jeray, S. Mehta, T. A. Einhorn, J. T. Watson, G. J. Della Rocca, K. Forbes, R. G. Steen, Bone fracture nonunion rate decreases with increasing age: A prospective inception cohort study. *Bone* **95**, 26–32 (2017).
65. R. Zura, Z. Xiong, T. Einhorn, J. T. Watson, R. F. Ostrum, M. J. Prayson, G. J. Della Rocca, S. Mehta, T. McKinley, Z. Wang, R. G. Steen, Epidemiology of fracture nonunion in 18 human bones. *JAMA Surg.* **151**, e162775 (2016).
66. L. A. Mills, S. A. Aitken, A. H. R. W. Simpson, The risk of non-union per fracture: Current myths and revised figures from a population of over 4 million adults. *Acta Orthop.* **88**, 434–439 (2017).
67. AO Foundation, AO Surgery Reference; https://surgeryreference.aofoundation.org/.
68. J. T. Lu, Y. J. Son, J. Lee, T. L. Jetton, M. Shiota, L. Moscoso, K. D. Niswender, A. D. Loewy, M. A. Magnuson, J. R. Sanes, R. B. Emeson, Mice lacking α-calcitonin gene-related peptide exhibit normal cardiovascular regulation and neuromuscular development. *Mol. Cell. Neurosci.* **14**, 99–120 (1999).

69. S. Jiang, P. Knapstein, A. Donat, S. Tsitsilonis, J. Keller, An optimized protocol for a standardized, femoral osteotomy model to study fracture healing in mice. *STAR Protoc.* **2**, 100798 (2021).
70. M. L. Bouxsein, S. K. Boyd, B. A. Christiansen, R. E. Guldberg, K. J. Jepsen, R. Müller, Guidelines for assessment of bone microstructure in rodents using micro-computed tomography. *J. Bone Miner. Res.* **25**, 1468–1486 (2010).
71. J. Luther, T. A. Yorgan, T. Rolvien, L. Ulsamer, T. Koehne, N. Liao, D. Keller, N. Vollersen, S. Teufel, M. Neven, S. Peters, M. Schweizer, A. Trumpp, S. Rosigkeit, E. Bockamp, S. Mundlos, U. Kornak, R. Oheim, M. Amling, T. Schinke, J.-P. David, Wnt1 is an Lrp5-independent bone-anabolic Wnt ligand. *Sci. Transl. Med.* **10**, eaau7137 (2018).
72. A. Dobin, C. A. Davis, F. Schlesinger, J. Drenkow, C. Zaleski, S. Jha, P. Batut, M. Chaisson, T. R. Gingeras, STAR: Ultrafast universal RNA-seq aligner. *Bioinformatics* **29**, 15–21 (2013).
73. Y. Liao, G. K. Smyth, W. Shi, featureCounts: An efficient general purpose program for assigning sequence reads to genomic features. *Bioinformatics* **30**, 923–930 (2014).
74. M. I. Love, W. Huber, S. Anders, Moderated estimation of fold change and dispersion for RNA-seq data with DESeq2. *Genome Biol.* **15**, 550 (2014).
75. J. Zyla, M. Marczyk, T. Domaszewska, S. H. E. Kaufmann, J. Polanska, J. Weiner, Gene set enrichment for reproducible science: Comparison of CERNO and eight other algorithms. *Bioinformatics* **35**, 5146–5154 (2019).
76. J. Appelt, S. Tsitsilonis, E. Otto, D. Jahn, P. Köhli, A. Baranowsky, S. Jiang, M. Fuchs, C. H. Bucher, G. N. Duda, K.-H. Frosch, J. Keller, Mice lacking the calcitonin receptor do not display improved bone healing. *Cells* **10**, 2304 (2021).
77. J. Keller, P. Catala-Lehnen, A. K. Huebner, A. Jeschke, T. Heckt, A. Lueth, M. Krause, T. Koehne, J. Albers, J. Schulze, S. Schilling, M. Haberland, H. Denninger, M. Neven, I. Hermans-Borgmeyer, T. Streichert, S. Breer, F. Barvencik, B. Levkau, B. Rathkolb, E. Wolf, J. Calzada-Wack, F. Neff, V. Gailus-Durner, H. Fuchs, M. H. de Angelis, S. Klutmann, E. Tsourdi, L. C. Hofbauer, B. Kleuser, J. Chun, T. Schinke, M. Amling, Calcitonin controls bone formation by inhibiting the release of sphingosine 1-phosphate from osteoclasts. *Nat. Commun.* **5**, 5215 (2014).

Acknowledgments: We thank O. Winter and A. Thieke for assistance with the undecalcified histology of unfractured bone samples. **Funding:** This study was funded by grants from the German Research Foundation (KE 2179/2-1 and KE 2179/2-3 to J.K.; TS 303/2-1 and TS 303/2-3 to S.T.). Partial support was provided by German Research Foundation project no. 427826188—SFB 1444 (to S.T.), the Einstein Center Regenerative Therapies of Charité—Universitätsmedizin Berlin (to D.J.), the Werner-Otto Foundation, Hamburg (to P.R.K.), and the Chinese Scholarship Council (to J.S. and W.X.). P.K. and F.G. are participants of the BIH-Charité Junior Clinician Scientist Program funded by the Charité—Universitätsmedizin Berlin and the Berlin Institute of Health. **Author contributions:** J.K. and S.T. were responsible for the study design. Coordination and supervision of all study-related activities as well as interpretation and conclusions of study data were performed by J.K.; D.J., E.O., and P.K. performed all experiments regarding the impact of TBI on fractured and unfractured bone. P.R.K. performed all surgeries, experiments, and data analyses regarding the in vivo role of ADRB2 in bone healing and remodeling. J.S. and A.B. conducted all in vitro experiments. C.G., M.F., S.J., M.R., C.E., J.A., J.W., A.R., W.X., and A.D. supported sampling, assessment, and analyses of in vivo and in vitro studies. Patient data were analyzed by F.G., L.R., and Q.K.; A.I., M.N.T., and D.B. performed analysis of RNA-seq data. J.K. and A.B. wrote the manuscript. Critical revision of the manuscript was performed by G.D., T.S., K.-H.F., and S.T. **Competing interests:** K.-H.F. is a senior consultant to Arthrex and receives royalties from a patent on the Arthrex patella plate. S.T. is a consultant to Johnson & Johnson. The other authors declare no competing interests. **Data and materials availability:** All data associated with this study are present in the paper or the Supplementary Materials. RNA-seq raw data have been deposited in GEO with accession number GSE253133.

Submitted 21 September 2023
Resubmitted 31 January 2024
Accepted 27 March 2024
Published 17 April 2024
10.1126/scitranslmed.adk9129

3. Zusammenfassung in deutscher Sprache

Mit zunehmendem Alter kommt es zu einem physiologischen Anstieg des Sympathikotonus und zu einer Abnahme der Knochenmasse im nicht-frakturierten Skelett. Vorherige Studien haben gezeigt, dass die durch Noradrenalin (Norepinephrin; NE) induzierte Abnahme der Knochenbildung und die Zunahme der Knochenresorption durch den beta2-adrenergen Rezeptor (Adrb2) vermittelt werden. Die Rolle von Adrb2 bei der Heilung eines gebrochenen Knochens war jedoch unklar. Um die Rolle von Adrb2 bei der Frakturheilung zu untersuchen, wurde in der vorliegenden Arbeit ein Mausmodell verwendet, bei dem eine Femurosteotomie mit einem Fixateur externe stabilisiert wird. Während Adrb2 bei jungen Mäusen mit niedrigem Sympathikotonus keine Rolle bei der Frakturheilung spielte, erwies sich Adrb2 bei adulten Mäusen mit erhöhtem Sympathikotonus als essenziell für die Knochenregeneration. Mechanistisch konnte gezeigt werden, dass Adrb2 die Expression des vaskulären endothelialen Wachstumsfaktors A (Vegfa) im Periost induziert und dadurch die Bildung von Typ-H-Blutgefäßen im Frakturkallus fördert, die die Neovaskularisation mit der Osteogenese koppeln. Die pharmakologische Blockade von Adrb2 mit Propranolol beeinträchtigte die Frakturheilung bei adulten Mäusen, während der Adrb2-Agonist Formoterol die Frakturheilung durch Regulierung der Neovaskularisation im Kallus förderte. Zusammenfassend zeigen diese Ergebnisse, dass das sympathische Nervensystem für die Knochenheilung unter hyperadrenergen Bedingungen, wie sie im höheren Lebensalter auftreten, von entscheidender Bedeutung ist. Darüber hinaus wurde Adrb2 als mögliches therapeutisches Ziel zur Verbesserung der Knochenheilung identifiziert.

4. Zusammenfassung in englischer Sprache

With advanced age, there is a physiological increase in sympathetic tone and a decrease in bone mass in the non-fractured skeleton. Previous studies have shown that the decrease in bone formation and the increase in bone resorption induced by noradrenaline (norepinephrine; NE) are mediated by the beta2-adrenergic receptor (Adrb2). However, the role of Adrb2 in the healing of fractured bone was unclear. To investigate the role of Adrb2 in fracture healing, the present study used a mouse model in which a femoral osteotomy is stabilized with an external fixator. While Adrb2 played no role in fracture healing in young mice with low sympathetic tone, Adrb2 was shown to be essential for bone regeneration in adult mice with increased sympathetic tone. Mechanistically, Adrb2 was shown to induce the expression of vascular endothelial growth factor A (Vegfa) in the periosteum, thereby promoting the formation of type-H blood vessels in the fracture callus that couple neovascularization with osteogenesis. Pharmacological blockade of Adrb2 with propranolol impaired fracture healing in adult mice, whereas the Adrb2 agonist formoterol promoted fracture healing by regulating neovascularization in the callus. In summary, these results show that the sympathetic nervous system is crucial for bone healing under hyperadrenergic conditions that occur in older age. Furthermore, Adrb2 was identified as a potential therapeutic target to improve bone healing.

5. Graphische Zusammenfassung

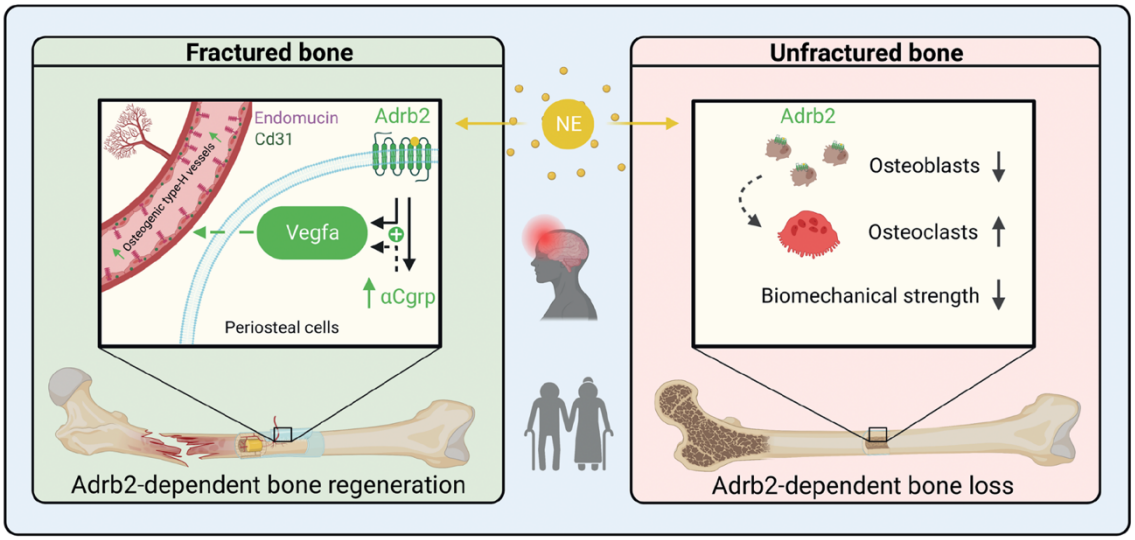

Abbildung 1 Übersicht über die Wirkung eines hyperadrenergen Zustandes (grau-blau) im fortgeschrittenen Alter oder nach Schädel-Hirn-Trauma auf das Skelett. Bei gleichzeitig vorliegendem Knochenbruch (grün), kommt es durch die Bindung von Norepinephrin an seinen Rezeptor Adrb2 zu einer vermehrten Vaskularisation des Kallus durch Typ-H-Gefäße. Im nicht-gebrochenen Knochen (rot) kommt es hingegen zu einem Knochenmasseverlust durch verringerte Osteoblastenaktivität bei erhöhter Osteoklastenaktivität. NE= Norepinephrin. Adrb2= beta2-adrenerger Rezeptor. aCGRP= Calcitonin-Gen-verwandtes Peptid alpha. Vegfa= Vaskulärer endothelialer Wachstumsfaktor A. CD31= Cluster of Differentiation 31. Abbildung basierend auf [45].

6. Literaturverzeichnis

1. Guntur, A. R. & Rosen, C. J. Bone as an endocrine organ. *Endocr Pract* **18**, 758–762 (2012).
2. Karsenty, G. & Khosla, S. The crosstalk between bone remodeling and energy metabolism: A translational perspective. *Cell Metab* **34**, 805–817 (2022).
3. Wildemann, B. *et al.* Non-union bone fractures. *Nat Rev Dis Primers* **7**, (1):57 (2021).
4. Schlickewei, C. W. *et al.* Current and future concepts for the treatment of impaired fracture healing. *Int J Mol Sci* **20**, 5805 (2019).
5. Kusumbe, A. P., Ramasamy, S. K. & Adams, R. H. Coupling of angiogenesis and osteogenesis by a specific vessel subtype in bone. *Nature* **507**, 323–328 (2014).
6. Compston, J. E., McClung, M. R. & Leslie, W. D. Osteoporosis. *Lancet* **393**, 364–376 (2019).
7. Wu, A. M. *et al.* Global, regional, and national burden of bone fractures in 204 countries and territories, 1990–2019: a systematic analysis from the Global Burden of Disease Study 2019. *Lancet Healthy Longev* **2**, e580–e592 (2021).
8. Russow, G. *et al.* Anabolic therapies in osteoporosis and bone regeneration. *Int J Mol Sci* **20**, (1):83 (2019).
9. Takeda, S. *et al.* Leptin regulates bone formation via the sympathetic nervous system. *Cell* **111**, 305–317 (2002).
10. Karsenty, G. & Khosla, S. The crosstalk between bone remodeling and energy metabolism: A translational perspective. *Cell Metabolism* vol. 34 805–817 Preprint at https://doi.org/10.1016/j.cmet.2022.04.010 (2022).
11. Jiang, S., Knapstein, P., Donat, A., Tsitsilonis, S. & Keller, J. An optimized protocol for a standardized, femoral osteotomy model to study fracture healing in mice. *STAR Protoc* **2**, (1):100798 (2021).
12. Balasubramanian, P., Hall, D. & Subramanian, M. Sympathetic nervous system as a target for aging and obesity-related cardiovascular diseases. *Geroscience* **41**, 13–24 (2019).
13. Stegen, S., van Gastel, N. & Carmeliet, G. Bringing new life to damaged bone: the importance of angiogenesis in bone repair and regeneration. *Bone* **70**, 19–27 (2015).
14. Wołowiec, Ł. *et al.* Beta-blockers in cardiac arrhythmias-Clinical pharmacologist's point of view. *Front Pharmacol* **13**, 1043714 (2022).
15. Ladage, D., Schwinger, R. H. G. & Brixius, K. Cardio-selective beta-blocker: pharmacological evidence and their influence on exercise capacity. *Cardiovasc Ther* **31**, 76–83 (2013).

16. Mintz, M. *et al.* Reducing the Risk of Mortality in Chronic Obstructive Pulmonary Disease With Pharmacotherapy: A Narrative Review. *Mayo Clin Proc* **98**, 301–315 (2023).
17. Smitham, P. *et al.* Low dose of propranolol does not affect rat osteotomy healing and callus strength. *J Orthop Res* **32**, 887–893 (2014).
18. Al-Subaie, A. E. *et al.* Propranolol enhances bone healing and implant osseointegration in rats tibiae. *J Clin Periodontol* **43**, 1160–1170 (2016).
19. Haffner-Luntzer, M. *et al.* Chronic psychosocial stress compromises the immune response and endochondral ossification during bone fracture healing via β-AR signaling. *Proc Natl Acad Sci U S A* **116**, 8615–8622 (2019).
20. Donat, A. *et al.* The selective norepinephrine reuptake inhibitor reboxetine promotes late-stage fracture healing in mice. *iScience* **26**, 107761 (2023).
21. Zhu, Y., Ma, Y. & Elefteriou, F. Cortical bone is an extraneuronal site of norepinephrine uptake in adult mice. *Bone Rep* **9**, 188–198 (2018).
22. Patro, B. P. *et al.* Traumatized periosteum: Its histology, viability, and clinical significance. *Orthop Rev (Pavia)* **14**, 30044 (2022).
23. Zura, R. *et al.* Bone fracture nonunion rate decreases with increasing age: A prospective inception cohort study. *Bone* **95**, 26–32 (2017).
24. Zura, R. *et al.* Epidemiology of fracture nonunion in 18 human bones. *JAMA Surg* **151**, 1–12 (2016).
25. Mills, L. A., Aitken, S. A., Hamish, A. & Simpson, R. W. The risk of non-union per fracture: current myths and revised fi gures from a population of over 4 million adults. *Acta Orthop* **88**, 434–439 (2017).
26. Munden, A. *et al.* Prospective study of infantile haemangiomas: incidence, clinical characteristics and association with placental anomalies. *Br J Dermatol* **170**, 907–913 (2014).
27. Léauté-Labrèze, C., Harper, J. I. & Hoeger, P. H. Infantile haemangioma. *Lancet* **390**, 85–94 (2017).
28. Chen, H. *et al.* Adrenergic signaling promotes angiogenesis through endothelial cell-tumor cell crosstalk. *Endocr Relat Cancer* **21**, 783–795 (2014).
29. Lu, K. *et al.* Suppression of beta 2 adrenergic receptor actions prevent UVB mediated cutaneous squamous cell tumorigenesis through inhibition of VEGF-A induced angiogenesis. *Mol Carcinog* **60**, 172–178 (2021).
30. Zahalka, A. H. *et al.* Adrenergic nerves activate an angio-metabolic switch in prostate cancer. *Science (1979)* **358**, 321–326 (2017).
31. Fredriksson, J. M., Lindquist, J. M., Bronnikov, G. E. & Nedergaard, J. Norepinephrine induces vascular endothelial growth factor gene expression in brown adipocytes through a beta -adrenoreceptor/cAMP/protein kinase A pathway involving Src but independently of Erk1/2. *J Biol Chem* **275**, 13802–13811 (2000).

32. Yamashita, H. *et al.* Norepinephrine stimulates the expression of fibroblast growth factor 2 in rat brown adipocyte primary culture. *Cell Growth Differ* **6**, 1457–1462 (1995).
33. Liu, W. *et al.* Traumatic brain injury stimulates sympathetic tone-mediated bone marrow myelopoiesis to favor fracture healing. *Signal Transduction and Targeted Therapy 2023 8:1* **8**, 1–17 (2023).
34. Song, Y. *et al.* The role of the hippocampus and the function of calcitonin gene-related peptide in the mechanism of traumatic brain injury accelerating fracture-healing. *Eur Rev Med Pharmacol Sci* **21**, 1522–1531 (2017).
35. Hinson, H. E. & Sheth, K. N. Manifestations of the hyperadrenergic state after acute brain injury. *Curr Opin Crit Care* **18**, 139–145 (2012).
36. Yang, T. Y., Wang, T. C., Tsai, Y. H. & Huang, K. C. The effects of an injury to the brain on bone healing and callus formation in young adults with fractures of the femoral shaft. *J Bone Joint Surg Br* **94**, 227–230 (2012).
37. Giannoudis, P. V. *et al.* Accelerated bone healing and excessive callus formation in patients with femoral fracture and head injury. *Injury* **37 Suppl 3**, S18-24 (2006).
38. Qian, J., Min, X., Wang, F., Xu, Y. & Fang, W. Paroxysmal Sympathetic Hyperactivity in Adult Patients with Brain Injury: A Systematic Review and Meta-Analysis. *World Neurosurg* **166**, 212–219 (2022).
39. Lecaillon, J. B., Kaiser, G., Palmisano, M., Morgan, J., Della Cioppa, G., Pharmacokinetics and tolerability of formoterol in healthy volunteers after a single high dose of Foradil dry powder Inhalation via aerolizer TM. *Eur J Clin Pharmacol* **55**, 131-8 (1999).
40. Hales, C. M., Servais, J., Martin, C. B. & Kohen, D. Prescription Drug Use Among Adults Aged 40-79 in the United States and Canada. *NCHS Data Brief* 1–8 (2019).
41. Steffenson, L. *et al.* Beta-blocker exposure is associated with nonunion in a geriatric cohort of 253,266 extremity fractures. *medRxiv* **2023.07.14**, 23292608 (2023).
42. Kajimura, D. *et al.* Genetic determination of the cellular basis of the sympathetic regulation of bone mass accrual. *Journal of Experimental Medicine* **208**, 841–851 (2011).
43. Elefteriou, F. *et al.* Leptin regulation of bone resorption by the sympathetic nervous system and CART. *Nature* **434**, 514–520 (2005).
44. Khosla, S. *et al.* Sympathetic β1-adrenergic signaling contributes to regulation of human bone metabolism. *J Clin Invest* **128**, 4832–4842 (2018).
45. Jahn, D. *et al.* Increased β2-adrenergic signaling promotes fracture healing through callus neovascularization in mice. *Sci Transl Med* **16**, 743 (2024).

7. Abkürzungsverzeichnis

Adrb1 ..... beta1-adrenerger Rezeptor
Adrb2 ..... beta2-adrenerger Rezeptor
Adrb3 ..... beta3-adrenerger Rezeptor
Hif1a ..... Hypoxie-induzierter Faktor 1-alpha
NE ..... Norepinephrin
SHT ..... Schädel-Hirn-Trauma
Slc6a2 ..... Solute Carrier Family 6 Member 2
SNS ..... Sympathisches Nervensystem
TRAP ..... Tartrat-resistente saure Phosphatase
Vegfa ..... Vaskulärer endothelialer Wachstumsfaktor A
WT ..... Wildtyp
µCT ..... mikro-Computertomographie

8. Abbildungsverzeichnis

9. Erklärung des Eigenanteils

Die vorliegende Arbeit wurde in der experimentellen Unfallchirurgie der Klinik und Poliklinik für Unfallchirurgie und Orthopädie des Universitätsklinikums Hamburg-Eppendorf in freundlicher Kooperation mit der Universitätsmedizin Charité in Berlin durchgeführt. Fachverantwortlicher Betreuer war hierbei Herr Prof. Dr. Dr. Johannes Keller. Die Konzeption und Planung der Studie erfolgten in Zusammenarbeit von Herrn Prof. Dr. Dr. Johannes Keller, Herrn PD. Dr. Serafeim Tsitsilonis und Frau Dr. Anke Baranowsky.

Eine umfangreiche Literaturrecherche und das Verfassen des Tierversuchsantrages N085/2020 wurde von mir in direkter Supervision durch die Betreuer durchgeführt. Alle Methoden bezüglich der *in vivo* Rolle von Adrb2 in der Knochenheilung und dem -umbau wurden eigenständig von mir unter Supervision durch die Projektleiter durchgeführt. Genauer beinhaltet dies alle operativen Eingriffe, täglichen Kontrollen, pharmakologischen Behandlungen, Euthanasie und die sich daran anschließenden Aufarbeitungen der Proben. Die Auswertung der morphologischen Parameter erfolgte mittels µCT und Histologie. Die Analyse zellulärer Parameter wurde an histologischen Schnitten (Movat-Pentachrome, von Kossa/ van Gieson, TRAP, Toloudin-Blau-Färbungen und Calcein-Inkorporation) durchgeführt. Die Anfertigung der mikroskopischen Präparate sowie der histologischen Färbungen erfolgte durch Unterstützung der technischen Assistentinnen C.E. und M.R. Ferner wurden durch mich die Analyse und Auswertung der immunohistochemischen Färbungen (Adrb2, Typ-H-Gefäße), die Genexperssionsanalysen mittels qRT-PCR nach RNA-Isolation und reverser Transkription in cDNA, ELISA Analysen von Cgrp, Vegfa und Normetanephrin und die Bestimmung des NE-Gehalts in nicht-frakturierten Knochen durchgeführt. Die Sichtung sowie statistische Auswertungen und Interpretation aller Ergebnisse erfolgte in enger Abstimmung mit den Projektleitern. Die Entscheidung über alle Abbildungen des finalen Manuskriptes erfolgte durch J.K. und A.B. und wurden durch mich mittels Adobe Illustrator zusammengestellt. Für die graphische Zusammenfassung nutze ich die BioRender-Homepage.

Alle relevanten *in vivo* Experimente und Analysen zur Rolle von Adrb2 im Knochenumbau und der Knochenregeneration, die in der oben aufgeführten Publikation beschrieben sind, wurden durch mich durchgeführt. In Kooperation mit anderen Wissenschaftlern und Wissenschaftlerinnen vom UKE und der Charité Berlin wurden darüber hinaus weiterführende Experimente durchgeführt, die ebenfalls im Rahmen der Publikation beschrieben sind. Frau D.J., E.O. und P.K. führten alle Experimente zu den Auswirkungen des SHT auf frakturierte und nicht-frakturierte Knochen durch. J.S. und

A.B. führten alle *in vitro* Experimente durch. Die Patientendaten wurden von F.G., L.R. und Q.K. analysiert; A.I., M.N.T. und D.B. führten die Analyse der RNA-Seq Daten durch. J.K. verfasste das Manuskript. Die kritische Überarbeitung des Manuskripts wurde von G.D., T.S., K.-H.F. und S.T. durchgeführt.

10. Eidesstattliche Versicherung

Ich versichere ausdrücklich, dass ich die Arbeit selbständig und ohne fremde Hilfe, insbesondere ohne entgeltliche Hilfe von Vermittlungs- und Beratungsdiensten, verfasst, andere als die von mir angegebenen Quellen und Hilfsmittel nicht benutzt und die aus den benutzten Werken wörtlich oder inhaltlich entnommenen Stellen einzeln nach Ausgabe (Auflage und Jahr des Erscheinens), Band und Seite des benutzten Werkes kenntlich gemacht habe. Das gilt insbesondere auch für alle Informationen aus Internetquellen.

Soweit beim Verfassen der Dissertation KI-basierte Tools („Chatbots“) verwendet wurden, versichere ich ausdrücklich, den daraus generierten Anteil deutlich kenntlich gemacht zu haben. Die „Stellungnahme des Präsidiums der Deutschen Forschungsgemeinschaft (DFG) zum Einfluss generativer Modelle für die Text- und Bilderstellung auf die Wissenschaften und das Förderhandeln der DFG“ aus September 2023 wurde dabei beachtet.

Ferner versichere ich, dass ich die Dissertation bisher nicht einem Fachvertreter an einer anderen Hochschule zur Überprüfung vorgelegt oder mich anderweitig um Zulassung zur Promotion beworben habe.

Ich erkläre mich damit einverstanden, dass meine Dissertation vom Dekanat der Medizinischen Fakultät mit einer gängigen Software zur Erkennung von Plagiaten überprüft werden kann.

Datum Unterschrift

11. Danksagung

Mein größter Dank richtet sich an meinen herausragenden Mentor und Doktorvater, Herrn Prof. Dr. Dr. Johannes Keller. Durch seine exzellente Betretung rund um die Uhr stellt er den fundamentalen Grundpfeiler meiner gesamten wissenschaftlichen Ausbildung und des sich nun daran anschließenden Werdegangs dar. Seine intrinsisch motivierte, positive und lösungsorientierte Art prägt meine Motivation für die Forschung nachhaltig.

Ebenso möchte ich ganz herzlichst Frau Dr. Anke Baranowsky danken. Ohne ihre großartige, tägliche Unterstützung und zentrale Expertise in allen Abschnitten des Forschungsprojektes wäre diese Arbeit nicht realisierbar gewesen.

Darüber hinaus gilt mein tiefer Dank dem gesamten Team der AG Keller, auf das ich mich zu jeder Tages- und Nachtzeit verlassen kann. Nur als gemeinsames Team ist solch ein Projekt zu bewältigen.

Danke an O. Winter und A. Thieke für die Unterstützung bei der Histologie der nicht gebrochenen Knochenproben.

Ich bedanke mich für die großzügige Unterstützung durch das Werner-Otto-Stipendium.

Besonderer Dank geht an meine mich stets unterstützende Familie: Paul-Georg, Sabine und Sophia. Ihr gebt mir den familiären Halt und Überblick während allen Höhen und Tiefen.

Ich widme die vorliegende Arbeit meinem Vater Prof. Dr. Paul-Georg Knapstein.

12. Lebenslauf

dr. med.-univ. Paul Richard Johannes Knapstein

Geboren am 23.06.1995 in Mainz (D)

Familienstand: ledig

Ausbildung

Juli 2024 Erfolgreicher Abschluss des Studiums der Humanmedizin (***gut***) und Approbation als Arzt durch die Freie und Hansestadt Hamburg

2024 Einreichung der Publikationspromotion mit dem Titel „Eine erhöhte beta2-adrenerge Signalübertragung fördert die Frakturheilung durch Kallus-Neovaskularisation in Mäusen“ zur Erlangung des Doktorgrades (Dr. med.) an der medizinischen Fakultät der Universität Hamburg

2023- 2024 Praktisches Jahr am Universitätsklinikum Hamburg-Eppendorf und der Universitätsmedizin in Mainz

2021 Veröffentlichung und mündliche Verteidigung der Diplomarbeit (***sehr gut***) mit dem Thema „Crosstalk of Brain and Bone-Clinical Observations and Their Molecular Bases“ zur Erlangung des Titels „dr. med.-univ.“

2020 Beginn der experimentellen Doktorarbeit am Universitätsklinikum Hamburg-Eppendorf in der experimentellen Unfallchirurgie. Zwei Forschungssemester in Vollzeit (Prof. Dr. Dr. J. Keller)

seit 2020 Promotionsstudent an der Universität Hamburg

2019-2021 Studentische Aushilfskraft auf den Interdisziplinären Intensivstationen am Universitätsklinikum Hamburg-Eppendorf

2019 Beginn des klinischen Studienabschnittes am Asklepios Campus in Hamburg (Wintersemester)

Juni 2019 Erfolgreicher Abschluss des ersten Abschnitts der ärztlichen Prüfung (***gut-sehr gut***)

2017 Beginn des Studiums der Humanmedizin an der Semmelweis Universität in Budapest (H)

2016 Zusatzqualifikation: A1-Ausbilder im Rettungsdienst

2015-2016 Ausbildung Rettungsdienst (***sehr gut***). Hauptberufstätig in der Notfallrettung (Rettungswagen und Notarzteinsatzfahrzeug der Rettungswache 02-ASB Mainz-Bingen)

2014-2017 Ehrenamtliche Versorgung von Obdachlosen und Flüchtlingen in Mainz mit der mobilen Ambulanz („Arztmobil“, Armut und Gesundheit in Deutschland e.V., Prof. Dr. G. Trabert)

2015 Allgemeine Hochschulreife am bischöflichen Gymnasium Theresianum in Mainz

2010-2011 Schulischer Auslandsaufenthalt in England (1 Jahr): The Oratory School, South Oxfordshire (UK)

Auszeichnungen

2024 New Investigator Award der European Calcified Tissue Society (ECTS)

2024 O&U Starting Grant des Universitätsklinikums Hamburg-Eppendorf

2024 Verlängerung des **Werner Otto Stipendiums** um ein weiteres Jahr

2023 Werner Otto Stipendium zur Förderung des medizinisch-wissenschaftlichen Nachwuchses an der Universität Hamburg

2021 Outstanding Reviewer Award der Society of Experimental Biology and Medicine (SEBM), supervised by Prof. Dr. Dr. J. Keller

Vorträge

2024 Vortrag mit dem Thema “The beta2-adrenoreceptor is essential for Bone Repair in Adult Mice” auf dem ECTS-Kongress in Marseille (F)

2024 Vortrag mit dem Thema “The beta2-adrenoreceptor Regulates Callus Neovascularization and Promotes Bone Repair in Adult Mice” vor dem Universitäts-Centrum für Orthopädie, Unfall-& Plastische Chirurgie des Universitätsklinikums Carl Gustav Carus in Dresden (PD Dr. Stefan Zwingenberger)

2022 Vortrag mit dem Thema „Impact of beta-adrenergic signaling on bone regeneration“ vor der Deutschen Wirbelsäulengesellschaft im Rahmen des „Satellitensymposium Spine Science“ in Berlin (Prof. Dr. P. Vajkcozy)

2022 Poster-Präsentation zu „Inactivation of beta2-adrenergic signaling improves bone regeneration“ auf dem ECTS- Kongress in Helsinki (FIN)

Unterschrift

13. Publikationsliste

2024 Jahn D*, **Knapstein PR***, Otto E*, Köhli P*, Sevecke J, Graef F, Graffmann C, Fuchs M, Jiang S, Rickert M, Erdmann C, Appelt J, Revend L, Küttner Q, Witte J, Rahmani A, Duda G, Xie W, Donat A, Schinke T, Ivanov A, Tchouto MN, Beule D, Frosch KH, Baranowsky A, Tsitsilonis S, Keller J. Increased β2-adrenergic signaling promotes fracture healing through callus neovascularization in mice. Science Translational Medicine 2024 Apr 17;16(743):eadk9129. (Impact Factor, IF =16.9). **contributed equally.* **Eigenanteil**: *siehe Punkt 9*

2024 Jiang S, Xie W, **Knapstein PR**, Donat A, Albertsen LC, Sevecke J, Erdmann C, Appelt J, Fuchs M, Hildebrandt A, Maleitzke T, Frosch KH, Baranowsky A, Keller J. Transcript-dependent effects of the CALCA gene on the progression of post-traumatic osteoarthritis in mice. Nature Communications Biology 2024 Feb 23;7(1):223. (IF=5.9). **Eigenanteil:** Assistenz bei chirurgischen Eingriffen, Euthanasierung der Versuchstiere, Probenaufarbeitung

2024 Xie W, Jiang S, Donat A, **Knapstein PR**, Albertsen LC, Kokot JL, Erdmann C, Rolvien T, Frosch KH, Baranowsky A, Keller J. Tranexamic Acid Attenuates the Progression of Posttraumatic Osteoarthritis in Mice. American Journal of Sports Medicine 2024 Mar;52(3):766-778. (IF=4.8). **Eigenanteil**: Assistenz bei chirurgischen Eingriffen, Euthanasierung der Versuchstiere, Probenaufarbeitung und Datenerhebung

2022 Buchkapitel: **Knapstein, PR**, Donat, A, Keller, J. Procalcitonin As a Biomarker and Mediator of Sepsis: Implications for Critical Care. In: Rajendram, R., Preedy, VR, Patel, VB (eds) Biomarkers in Trauma, Injury and Critical Care. Biomarkers in Disease: Methods, Discoveries and Applications. Nature-Springer Verlag 2022. **Eigenanteil**: Konzeption und Verfassung des Manuskriptes, Literaturrecherche, Erstellung der Abbildungen

2022 Grewe JM, **Knapstein PR**, Donat A, Jiang S, Smit DJ, Xie W, Keller J. The role of sphingosine-1-phosphate in bone remodeling and osteoporosis. Nature Bone Research 2022 Apr 8;10(1):34. (IF= 13.5). **Eigenanteil**: Literaturrecherche, Durchsicht und Überarbeitung des Manuskriptes und der Abbildungen

2022 Messerer DAC, Datzmann T, Baranowsky A, Peschel L, Hoffmann A, Gröger M, Amling M, Wepler M, Nussbaum BL, Jiang S, **Knapstein PR**, Donat A, Calzia E, Radermacher P, Keller J. Systemic calcitonin gene-related peptide receptor antagonism decreases survival in a porcine model of polymicrobial sepsis: blinded randomised controlled trial. British Journal of Anaesthesia 2022 May; 128(5):864-873. (IF= 9.2). **Eigenanteil**: Probenaufarbeitung und Datenerhebung

2022 Baranowsky A, Jahn D, Jiang S, Yorgan T, Ludewig P, Appelt J, Albrecht KK, Otto E, **Knapstein PR**, Donat A, Winneberger J, Rosenthal L, Köhli P, Erdmann C, Fuchs M,

Frosch KH, Tsitsilonis S, Amling M, Schinke T, Keller J. Procalcitonin is expressed in osteoblasts and limits bone resorption through inhibition of macrophage migration during intermittent PTH treatment. Bone Research 2022 Jan 27;10(1):9. (IF= 13.5). **Eigenanteil**: Euthanasierung der Versuchstiere, Probenaufarbeitung und Datenerhebung, *in vitro* Experimente

2021 Jiang S, **Knapstein PR**, Donat A, Tsitsilonis S, Keller J. An optimized protocol for a standardized, femoral osteotomy model to study fracture healing in mice. Cell Press STAR Protocol 2021 Sep 8;2(3):100798. (IF= 1.3). **Eigenanteil**: Assistenz bei chirurgischen Eingriffen, Erstellung der Abbildungen, Literaturrecherche, Durchsicht und Überarbeitung des Manuskriptes und der Abbildungen

2021 Donat A, **Knapstein PR**, Jiang S, Baranowsky A, Ballhause TM, Frosch KH, Keller J. Glucose Metabolism in Osteoblasts in Healthy and Pathophysiological Conditions. International Journal of Molecular Sciences 2021 Apr 16;22(8):4120. (IF= 6.2). **Eigenanteil**: Literaturrecherche, Erstellung der Abbildungen, Durchsicht und Überarbeitung des Manuskriptes

2020 Otto E*****, **Knapstein PR***, Jahn D, Appelt J, Frosch KH, Tsitsilonis S, Keller J. Crosstalk of Brain and Bone-Clinical Observations and Their Molecular Bases. International Journal of Molecular Sciences 2020 Jul 13;21(14):4946. (IF=6.2). *******contributed equally.* **Eigenanteil**: Erstellung des Manuskriptes und der Abbildungen, Literaturrecherche

Kumulativer IF= 77.5